Wireless coverage in the public transportation system

AALBORG UNIVERSITY
STUDENT REPORT

Aalborg University
Group 15gr1055 - Wireless Communication

AALBORG UNIVERSITY
STUDENT REPORT

Department of Electronic Systems
Fredrik Bajers Vej 7 B
9220 Aalborg Ø
Tlf.: 9940 8600
http://es.aau.dk

Title: Wireless coverage in the public transportation system

Project Periode:
Master Thesis

Project Group:
15gr1055

Participant:
Jesper Nysted Andersen

Supervisors:
Troels B. Sørensen
Ignacio Rodriguez Larrad

Copies: 4

Page Numbers:

Date of Completion. Date 3/6-15

Abstract:

This project have investigated the coverage along the railway to find the main reason for the poor coverage when traveling by train. In the report there have been theorectic work to investigate the coverage along the railway. By investigating propagation models and simulation of the receive power along the railway. A set of measurements have been used to find a value for the penetration loss into the train.

Contents

Chapter 1

Introduction

1.1 Introduction

Wireless networks and ubiquitous wireless coverage is essential for a modern society. The public expectation and dependence of wireless networks to be available is increasing as the number of devices and traffic is growing [1, 2]. Different wireless network exist, but especially the cellular network is widely used with almost 7 billion mobile subscribers world wide [3]. The cellular network has to offer great capacity, coverage and quality for the users, which sets requirement for the planning of the network. The trade off in the network can usually be seen in areas with low population density or in case of unexpected traffic and/or number of users.

The coverage is depending on the placement and configuration of the Base Stations (BSs). For most urban areas, the coverage expectation is fulfilled due to the high density of wireless infrastructure. In rural areas, the situation is different due to the much sparser wireless infrastructure. Operators are less inclined to build out their infrastructure in rural areas due to the low population density. Other factors also have an impact in the coverage, this could be obstacles in the way of the signal path, building material, i.e. penetration loss, fades because of multipath, etc.

In Denmark the outdoor coverage of the cellular network is 99 % for 497 of the 586 postal codes, according to the Danish Business Authority [4]. But even with high percentage coverage in Denmark there seems to be lack of coverage in some situations. An example of this is the cellular coverage inside the Danish trains which have been debated over several years. With the train operator on one side arguing that the cellular network is lacking in coverage for certain areas. The cellular operators on the other side stating that it is the penetration into the train that is the problem. From the material found the first report of how to solve the mobile reception problems that occur inside the train is in an article from 2007 [5]. The article states that the Danish train company, DSB, have an agreement in the making with the cellular operators of how to solve the problem. But the debate carries on and the problem have not been fixed yet. The main content of the articles will be presented in the following section.

1.2 Debate of the coverage inside the train

The debate starts in 2007 with an article in the Danish newspaper "Ingeniøren"[5], described the dilemma with poor mobile coverage. The spoke person for the stretch between Helsingør-Copenhagen, Klavs Kofod, states that on particular places along the tracks there are no cellular coverage [5]. The article also discusses the structure of the train as a problem and states they are constructed as a Faraday-cage, where even the windows have metal threads inside them. Which is the reason that DSB is trying to get a deal with the cellular operators. Such a deal is a must because DSB made a deal when they won the election for the Oresund traffic. The solution they suggest is cellular repeaters. DSB also invest in Wi-Fi coverage in the train, at first in the trains between Korsør-Copenhagen. The hot spots is made together with TDC.

Then in 2010 an article describes the problems with the IC4 trains in particular [6]. In this article the problem is relates to how the new train is constructed. Because of all the electronic to control e.g. door, lighting etc. that needs to be protected for safety reasons. The trains have to be protected against electromagnetic radiation, this protection also cover some of the frequencies used by the cellular network. To lower the pressure change in the trains makes them more airtight than before, because they need to travel in the new tunnels. The windows are discussed as well as being a problem. The new windows are created so they have a higher breaking strength and have several layers so the sun doesn't come in and the heat stays inside[7]. Torben Kronstam, Head of the IC4 Program, also specifies that it is not only a problem for DSB but also the cellular operators. DSB is looking at different solutions and repeaters are mentioned as one of the solution, it is also stated that the agreement they where looking at in 2007 with repeaters wasn't completed. And Claus Klitholm, head of business development in DSB cannot say anything about when the installation is expected but states that it will be in the near future. Analyst John Strand is not impressed that the problems have not been solved and doesn't have much to say about how DSB handles the IC4 Trains. He also states that this is not isolated to the trains in Denmark but countries like Switzerland and Germany already have solved this with the use of repeaters.

In an article Maj 2012 [8] it is stated that DSB is close to a deal with the four major cellular operators in Denmark for delivery of cellular repeaters for all trains. And DSB will also make an upgrade of the Wi-Fi network in the trains so they support three time as much data up to 21 Mbit/s. Then in December 2012 another article [9] describes the problems with the Wi-Fi in the trains as being impossible to use related to the capacity. DSB states that this is due to delivery problems of hardware. The problems with the cellular network also seem to still be a problem and they have installed repeaters in the trains.

In January 2013 [10] they are still discussing to install 260 repeaters in the trains. And the reports of coverage problem from 2007 is supplied by reports by the employees at DSB, which have created a list with stretches that have poor cellular coverage. The list is given in an article from 2013 by computer world [11] and the locations are plotted in figure 1.1. Because the list is given by the employees at DSB the result can be impacted by the fact that this is the stretches where the personal have time to use there devices. The places is also located along the intercity train route, and the smaller local routes is therefore left out.

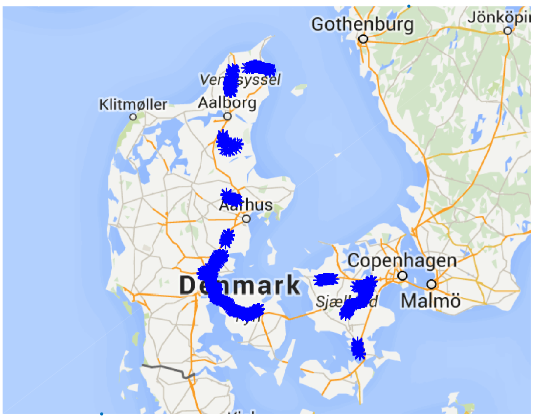

Figure 1.1: Map showing the worst locations according to DSB staff in 2013 [11].

18. of May 2015 a contract between Banedanmark, DSB, Arriva and the four major cellular operator in Denmark have made a contract [12]. The contract gives the cellular operator permission to use the BSs that belong to Banedanmark and install repeaters inside the trains. They expect that they will have a solution ready in three year. In the article it is stated that the first assignment is to map the coverage along the railway, as to locate the concrete upgrades.

As the discussion have continued for 8 years at this point and they still haven't investigated what is the cause of the poor coverage along the railway. A investigation of the coverage along the railway will be described in this report.

1.3 Problem definition

Problems with the coverage of the mobile signal inside the train have been a problem for several years according to the discussion that have been going on in the articles. As stated in the last article the problem with the coverage is not determined and needs to be investigated. In this project an initial investigation of the coverage along the railway will be given. The dilemmas that could prove to be important for the coverage could be the:

- BS placement along the railway

- Penetration loss into the train
- Obstacles close to the railway
- Handover

This report will focus on the coverage of the BSs compared with the location of the railway. A penetration loss into the train will also be investigated as to locate a potential problem. The focus of the project lead to the problem definition:

> *"Is the BS positions creating problems for the received signal inside a train or is the train itself the main problem?"*

The structure of the project start with an chapter of the mobile coverage that leads to a link budget. Chapter 3 compares different propagation models for the use in the simulation in chapter 4. The simulation predict the theoretic coverage of the different model along the railway. In chapter 5 investigation of some measurements find a relation between the measured data outside of the train with data inside of the train.

Chapter 2

Mobile coverage

The debate in chapter 1, between DSB and the cellular operators highlights a general problem with the coverage inside the train. The lack of coverage can be seen in the feedback from staff and commuters. The discussion also leads up to the lack of knowledge as to what the actual problem is. In this chapter a fundamental understanding of the mobile coverage will be given and end up with a link budget for the BS. The power received, which is affected by the propagation through the environment and the transmitted power, determines the mobile coverage. The power received, [dBm], P_r, can be expressed as shown in equation 2.1.

$$P_r[dBm] = P_t[dBm] - P_L[dB] \qquad [dBm] \quad (2.1)$$

Where P_t is the power transmitted, [dBm] and P_L is the path loss, [dB]. The path loss in this case is the propagation of the signal through the environment. A full description of the propagation environment is quite complex and every information about it is difficult or impossible to obtain. The path loss is usually obtain by approximations either by solving Maxwell's equations, ray-tracing or simple propagation models, either statistical or empirical. In chapter 3 further description of the propagation model will be given. This chapter will start on describing the propagation environment, continuing with penetration into the train in section 2.2. In section 2.1.3 describing the antenna characteristic with a focus on the gain of the antenna. Setting up the coverage definitions in section 2.3 and ending up with a link budget in section 2.4.

2.1 Propagation

The propagation of radio signals through an environment is affected by several factors e.g. distance, reflections, scattering, diffraction's etc. In this sections a general look at the propagation environment in relation to the power received. Starting with an example showing the the dependence on distance and frequency in free-space.

2.1.1 Free-space propagation

Free-space propagation is describing the case where the transmitter and receiver is in Line-Of-Sight (LOS) of each other and there are no obstacles to reflect, scatter and diffract the signal. The power received at a given distance and frequency can be determined based on equation 2.2

which in general is referred to as the free-space path loss.

$$P_r[dBm] = P_t[dBm] + 10log_{10}\left(\frac{\sqrt{G_l}\lambda}{4\pi d}\right)^2 \qquad [dBm] \quad (2.2)$$

Where $P_{received}$ is the power received, $P_{transmitted}$ is the power transmitted, G_l is the product of the receive and transmit antenna field radiation patterns in the LOS direction, [.], λ is the wavelength and d is the distance between transmitter and receiver. The wavelength, λ is defined as in equation 2.3.

$$\lambda = \frac{c}{f_c} \qquad [m] \quad (2.3)$$

Where c is the speed of light and f_c is the carrier frequency. As the carrier frequency increases the wavelength decreases and with a constant G_l the power received will be lower. The power also decreases with the square of the distance. In figure 2.4 the behaviour of the received power with $P_t = 0$ [dBm], $G_l = 1$, distance ranging from 1 m to 5 km and two different carrier frequencies. The carrier frequency is set to 900 MHz and 2100 MHz which is two of the regular cellular frequencies used in Denmark.

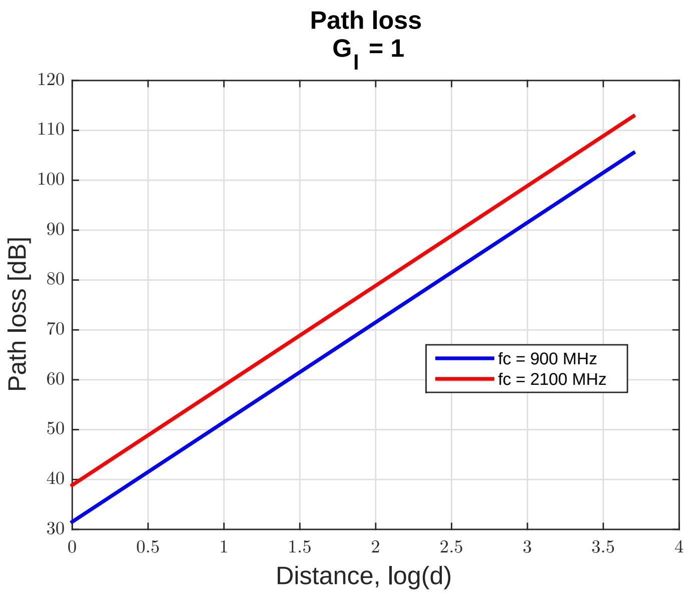

Figure 2.1: Power received for $f_c = 900$ MHz and $f_c = 2100$ MHz, $G_l = 1$, $P_t = 0$ [dBm] and the distance ranging from 1 m to 5 km

If the signal is following the free-space propagation and the signal attenuates with distance and frequency. Then the difference between a frequency of 900 MHz and 2100 MHz is 7.36 [dB]. It can be noticed that increasing the frequency decreases the power received. Equation 2.1 can be rewritten to equation 2.4, a function depending on the distance as the carrier frequency is often determined beforehand and constant.

$$P_r(d)[dBm] = P_t[dBm] - P_L(d)[dB] \qquad [dBm] \quad (2.4)$$

Free-space conditions is difficult to achieve in the mobile network, because of the ground and obstacles on the ground e.g. buildings, trees etc. The obstacles in the path way produces additional copies of the transmitted signal known as multipath signals. Multipath signals can both increase and decrease the power of the signal at the receiver, as the received signal will be the sum of the received multipath signal. The multipath propagation can be solved using Maxwell's equations, with appropriate boundary conditions, or with ray tracing techniques. For analysis usage these methods can be computational and time consuming and often empirical propagation models is used to give a indications of the path loss in the environment. In the rest of this chapter the loss of the model will be described with L_{model} as no specific model is given. In chapter 3 a overview of different models is given that is used in the simulations.

2.1.2 Shadow fading

A limiting factor to the propagation models is the unknown factors from changes in scattering objects and reflections e.g. moving objects. These changes in the propagation environment is random and is often modelled statistically. A common model used for these random changes is the log-normal shadowing. The shadowing can be superimposed onto the model for the path loss, where the path loss model determines the average dB path loss and the shadow fading is creating variations around this with a mean of 0. This means that the expression for the path loss P_L in equation 2.4 can be written as equation 2.5

$$P_L(d)[dB] = L_{model}(d)[dB] - \chi_{dB} \qquad [dB] \quad (2.5)$$

Where L_{model} is the path loss according to the chosen model and χ_{dB} is log-normal fading, $N(0,\sigma_{\chi_{dB}})$. This random part included in the path loss have impact on the receive power at any given distance. This will have an impact on the coverage of the mobile network and will be discussed further in section 2.3. In the free space propagation model the gain was neglected as the antenna was treated as omni-directional, but the antenna is important when it comes to the mobile coverage. In section 2.1.3 an actual antenna used in the mobile network will be described.

2.1.3 Antenna characteristic

In this section a description of the antenna characteristic will be presented. An antenna is normally characterised with a representation of the magnitude of either the electric or magnetic field or the power pattern. The pattern is used to describe the radiation density, radiation intensity, field strength, directional properties. Another parameter used in describing an antenna is the efficiency of the antenna and together with the directional properties can give an actually gain of the antenna. In this section the focus will be on the gain of the antenna with a description of the needed pattern characteristic. The absolute gain of an antenna is defined as in equation 2.6

$$G(\theta,\phi) = e_0 D(\theta,\phi) \tag{2.6}$$

Where e_0 is the total antenna efficiency and $D(\theta,\phi)$ is the directivity. θ,ϕ is referring to the angles according to the elevation plane and the azimuth plane. The total antenna efficiency is taking into account the losses because of the structure or at the input terminals. The efficiency can be described as in equation 2.7

$$e_0 = e_r e_c e_d \tag{2.7}$$

Where e_r is the reflection-, e_c the conduction- and e_d the dielectric efficiency. The directivity as defined by IEEE

> ”The ratio of the radiation intensity in a given direction from the antenna to the radiation intensity averaged over all directions[13]”

and expressed in equation 2.8

$$D = \frac{U}{U_0} \tag{2.8}$$

Where U is the radiation intensity in a given direction and U_0 is the radiation intensity of an isotropic source. To evaluate the gain of an antenna data have been given for the Kathrein 1710-2690 antenna[14]. A two dimensional pattern have been given for both the azimuth and the elevation pattern. The patterns exist for six different tilt options for the antenna, 0,2,4,6,8,10. In figure 2.2 the antenna pattern is shown for the azimuth in figure 2.2a and the elevation pattern in figure 2.2b for the case where the tilt = 0 and 6.

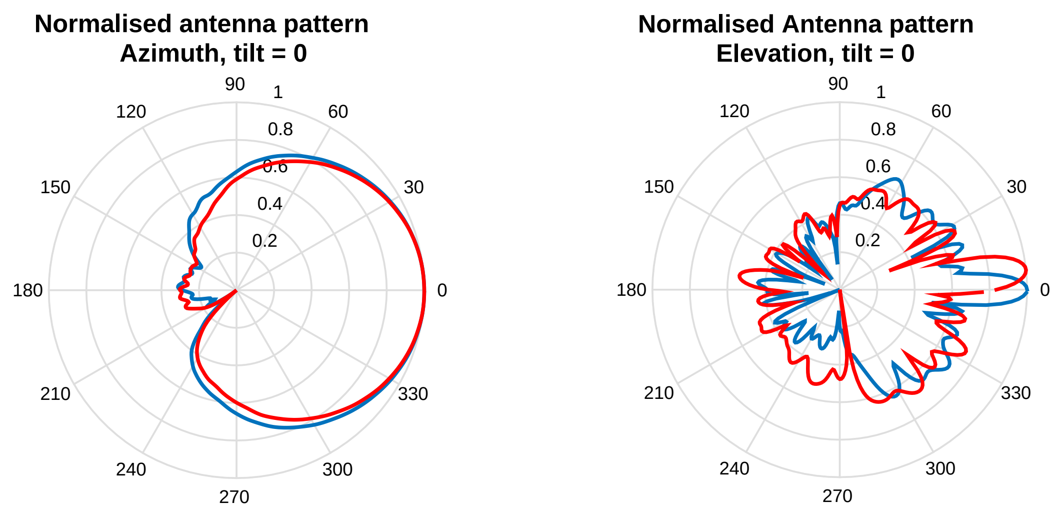

(a) Normalised antenna pattern in the azimuth plane

(b) Normalised antenna pattern in the elevation plane

Figure 2.2

The calculation of the gain is described in the simulation description in section 4.1.1. In the next section the penetration loss into the train will be discussed.

2.2 Penetration into the train

The penetration loss is considered in several cases e.g. penetration into buildings, the loss can have a high impact on the coverage of the signal. The penetration into buildings is dependent on several factor e.g. material, structure, incidence angle etc [15]. Little material have been found for the penetration loss into train. But one article [16] have a short section describing measurement with different result for the penetration loss. The article states penetration loss ranging from 0 - 22 dB and even higher values if the train have metallised windows. The article described that the incidence angle have an impact of the penetration loss. The case is illustrated in figure 2.3. This idea will also be used to investigate the penetration loss from the measurements in chapter 5. The angle of incidence is measured from the normal incidence to the surface of the object. For this case to hold the signal have to be dominated by one path to the object.

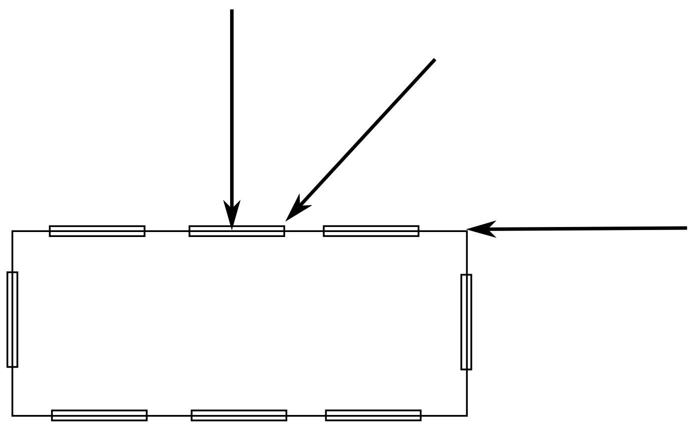

Figure 2.3: Plot of a train seen from above, with three different rays onto the structure of the train

2.3 Cell coverage

In this section a description of the cell coverage will be given for the mobile network.

In figure 2.4 a single omni-directional antenna inside a grey area is shown. Two identities of coverage probabilities could be determined when also considering the fading parameter, rim coverage probability and coverage area probability.

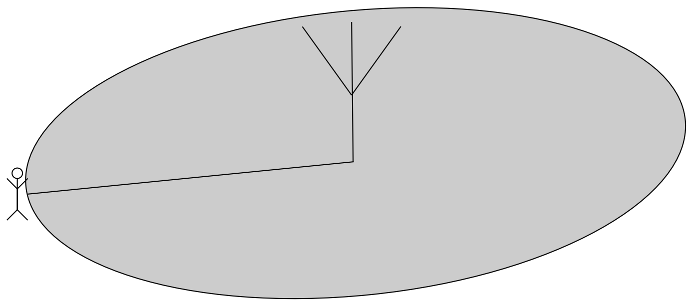

Figure 2.4: Single cell coverage

The rim coverage probability is the probability that the power level is higher than a threshold value, κ, at a given distance d from the antenna. The rim coverage probability can be defined as in equation 2.9.

$$P[P_r(d) > \kappa] = Q\left(\frac{\kappa - \overline{P}_r(d)}{\sigma_{\chi_{dB}}}\right) \tag{2.9}$$

Where κ is the required power level and Q is the Q-function. The area coverage probability is the probability that at any position inside a given area the power level is higher than the threshold value, κ. The area coverage probability can be expressed as in equation 2.10.

$$P^{\kappa} = \frac{1}{\pi d_{max}^2} \oint P[P_r(d) > \kappa] dA \tag{2.10}$$

Where P^{κ} is the area probability and d_{max} is the distance at the cell boundary.

The probabilities are usually used as a minimum requirement for the coverage, because it is impossible to achieve 100 % coverage.

2.4 Link budget

In this section the link budget is given for the downlink. In table **??** the details for the BS is given. The transmit power of the BS is based on the value for different base stations along the railway. The antenna gain and body loss values is found in an 3GPP technical report [17]. The maximum path loss can be found by analysing the link budget, the link budget is shown in table 2.1.

Index	**Link budget**	**Description**	**Value**
Transmitter BS			
(1)	Transmit power	P_t	43 [dBm]
(2)	Ant. gain	G_t	16 [dBi]
(3)	Body loss trainsmitter	L^{t}_{Body}	3 [dB]
(4)	Total power BS	EIRP	56 [dBm]
Receiver User Equipment (UE)			
(5)	Noise figure	NF	7 [dB]
(6)	Antenna gain	G_r	0 [dBi]
(7)	Diversity gain	G_D	-3 [dB]
(8)	Body loss receiver	L^{r}_{Body}	1 [dB]
(9)	Thermal noise	kTb	-107 [dBm]
(10)	Sensitivity		-102 [dB]
Detection			
(11)	Signal Noise Ratio	SNR	5 [dB]
Load			
(12)	Interference margin	L_{im}	3 [dB]
(13)	Fast fading margin	L_{ff}	2 [dB]
(14)	Train penetration loss	L_{TP}	0-22 [dB]
(15)Allowed propagation loss	L_{PL}	148 [dB]	

Table 2.1: Link budget - details

The transmitter characteristic is given as the EIRP and is calculated as stated in equation

2.11 and result shown in 2.12.

$$EIRP = (1) + (2) - (3) \tag{2.11}$$

$$(4) = 56 \qquad [dBm] \tag{2.12}$$

The receiver characteristic is given as the sensitivity and is calculated as stated in equation 2.13 and result shown in 2.14.

$$sensitivity = (5) + (6) + (7) + (8) + (9) \tag{2.13}$$

$$(10) = -102 \qquad [dBm] \tag{2.14}$$

The allowed total propagation loss is then calculated as in equation 2.17 and result shown in 2.14.

$$L_{PL} = (4) - ((10) + (11) + (12) + (13) + (14)) \tag{2.15}$$

$$(10) = 148 \qquad [dBm] \tag{2.16}$$

where (14) the train penetration loss is 0, if the train penetration loss is instead 22 the result would instead be as in equation 2.18

$$L_{PL} = 126 \qquad [dBm] \tag{2.17}$$

$$\tag{2.18}$$

In this chapter a description of the propagation environment have been given along with a description of the coverage probability for the rim and the area. A penetration loss for the train have been given and in the end a link budget have been setup. In chapter 3 different propagation model will be described for use in the simulations and to given and expected coverage distance according to the link budget.

Chapter 3

Propagation models

In this chapter different propagation models will be given, which will be used for simulations in chapter 4. In chapter 1 the debate lead to the fact that the coverage problem seem to be worst in the rural areas. The propagation models used will be chosen based on this fact. In section 2.1 a review of the propagation environment was given. The free-space path loss model was given as an example of how the distance and frequency effects the attenuation. Chapter 2 also gave an overview of how the coverage is defined and ended up with a link budget. This will be used to compare the different models that will be discussed in this chapter. In the following sections different models will be investigated starting with the simplified path loss model in section 3.1, the Hata model in section 3.2 and the RMa model in section 3.3. In section 3.4 the different models will be compared.

3.1 Simplified path loss model

The simplified path loss model is often used as an foundation for other models. The model is simple to implement and can be used to give a rough estimate. The simplified path loss model is shown in equation 3.1.

$$PL_{Simplified} = 10\gamma log_{10}\left(\frac{d}{d_0}\right) - K_{dB} \qquad [dB] \quad (3.1)$$

Where γ is the path loss exponent, [.], $d0$ is the reference distance, [m] and K is a constant dependent on antenna characteristics and channel attenuation, [.], shown in equation 3.2

$$K_{dB} = 20log_{10}\left(\frac{\lambda}{4\pi d_0}\right) \qquad [.] \quad (3.2)$$

For a $\gamma = 2$ the simplified path loss approximately follows the free-space path loss, [.] and for a $\gamma = 4$ the two ray model.

3.2 Hata model

The Hata model [18] is an empirical model based on measurements performed by Okumura. The measurements was between a BS and a Mobile Station (MS) and where performed in Tokyo. Okumura created empirical curves for different parameters. These curves was converted into a closed form formula, known as the Hata model. The formula for urban areas is shown in equation 3.3 [19].

$$PL_{Hata}^{urban} = 69.55 + 26.16log_{10}(f_c) - 13.82log_{10}(h_t) - a(h_r) + (44.9 - 6.55log_{10}(h_t))log_{10}(d) \quad [dB] \tag{3.3}$$

Where f_c is the carrier frequency, [Hz], h_t is the height of the transmitter, [m], h_r the height of the transmitter, [m], d is the distance between transmitter and receiver and a is a correction factor for the height of the receiver based on the size of the coverage area, [dB] and is shown in equation 3.4 for small to medium size cities.

$$a(h_r) = 0.8 + (1.1log_{10}(f_c) - 0.7)h_r - 1.56log_{10}(f_c) \tag{3.4}$$

The Hata model is made for urban areas and is most suite for distances between 1-10 km and carrier frequencies from 150-1500 MHz. A receiver height of 1-10 m and a base station height of 30 -200 m. The model is extended into a rural propagation model, as shown in equation 3.5[18].

$$PL_{Hata}^{rural} = PL_{Hata}^{urban} - 4.78(log_{10}(f_c))^2 + 18.33log_{10}(f_c) - 40.94 \quad [dB] \tag{3.5}$$

The Hata model is underestimating for higher frequencies and an extension was added by the European study committee, known as the COST 231 extension. The extended Hata model is shown in equation 3.6.

$$PL_{Hata}^{extended} = 46.3 + 33.9log_{10}(f_c) - 13.82log_{10}(h_t) - a(h_r) + (44.9 - 6.55log_{10}(h_t))log_{10}(d) \tag{3.6}$$

The extended model have the following parameters, 1.5 [GHz] $< f_c <$ 2 [GHz] and 1 [km] $< d$ $<$ 20 [km]. The Hata models are most suited for larger cell sizes, which also can be seen in the distance parameters.

3.3 3GPP Rural Macro

The 3GPP have set up path loss models for use in different scenarios [20] the model is based on measurements. A model for Rural Macro-cell (RMa) is outlined in this section. The RMa is split into a LOS and a No Line-Of-Sight (NLOS). The frequency range of the model is from 450 [MHz] to 6 [GHz] no matter if it is the LOS or NLOS.

3.3.1 Rural Macro for LOS

For the LOS case the model resembles the two ray model and is split into two parts. In equation 3.7 the path loss for the LOS is shown for distances d $< d_{BP}$, and in equation 3.8 it is shown for d ¿ d_{BP}. d_{BP} is the break point distance, [m], which also can be seen in figure 3.1.

$$PL_{RMa1}^{LOS} = 20log_{10}\left(\frac{40\pi d f_c}{3}\right) + min(0.03h_b^{1.72},10)log_{10}(d) - min(0.044h_b^{1.72},14.77) + 0.002log_{10}d \tag{3.7}$$

Where h_b is the average building height, [m]. The standard deviation of the shadow fading is given as $\sigma = 4$ for PL_{RMa1}^{LOS}.

$$PL_{RMa2}^{LOS} = PL_{RMa1}^{LOS}(d_{BP}) + 40log_{10}\left(\frac{d}{d_{BP}}\right) \tag{3.8}$$

The standard deviation of the shadow fading is given as $\sigma = 6$ for PL_{RMa2}^{LOS}. The break point distance is calculated based on equation 3.9

$$d_{BP} = 2\pi h_t h_r f_c/c \tag{3.9}$$

The application range for both cases of the LOS is 5 [m] $< h_b <$ 50 [m], 5 [m] $< W <$ 50 [m], 10 [m] $< h_t <$ 150 [m], 1 [m] $< h_r <$ 10 [m] and 10 [m] $< d <$ 10000 [m].

3.3.2 Rural Macro for NLOS

For the NLOS case the rural macro model is given as in equation 3.10.

$$\begin{aligned} PL_{RMa}^{NLOS} = & 161.04 - 7.1log_{10}(W) + 7.5log_{10}(h_b)... \\ & - (24.37 - 3.7(h_b/h_t))^2 log_{10}(h_t)... \\ & + (43.42 - 3.1log_{10}(h_t)(log_{10}(d) - 3)... \\ & + 20log_{10}(f_c) - (3.2(log_{10}(11.75h_r)))^2 - 4.97 \end{aligned} \tag{3.10}$$

Where W is the street width, [m] and the standard deviation of the shadow fading is given as $\sigma = 8$ for PL_{RMa}^{NLOS}. The application range the NLOS is 5 [m] $< h_b <$ 50 [m], 5 [m] $< W <$ 50 [m], 10 [m] $< h_t <$ 150 [m], 1 [m] $< h_r <$ 10 [m] and 10 [m] $< d <$ 5000 [m].

3.4 Comparison of the models

In this section the models will be compared. In table 3.1 the variables used in the different models is shown. In table 3.2 variable used in the RM model is given.

In figure 3.1 the path loss is plotted for the for the different model based on the variables given in table 3.1. Further more the simplified path loss model have been plotted with a $\gamma = 2$ and $\gamma = 4$.

General variables		
f_c	900	[MHz]
d_{min}	10	[m]
d_{max}	5000	[m]
h_t	30	[m]
h_r	1.5	[m]

Table 3.1: General variable between the four models

RM variables		
h_b	5	[m]
W	20	[m]

Table 3.2: Variable for the two RM models

3.4.1 Coverage distance

The coverage distance for the different model can be found by solving the path loss equations for the distance d. The maximum path loss was given in the link budget in section 2.4. Solving equation 3.1 for the distance, d, and $d_0 = 1$, gives equation 3.11.

$$d_{Simplified} = 10^{\frac{PL_{Simplified} - K_{dB}}{10\gamma}} \quad [m] \tag{3.11}$$

For the rural HATA model equation 3.5 can be rewritten to equation 3.12.

$$PL_{Hata}^{urban} = PL_{Hata}^{rural} + 4.78(log_{10}(f_c))^2 - 18.33log_{10}(f_c) + 40.94 \quad [dB] \tag{3.12}$$

Equation 3.12 can then be inserted in equation 3.3 which can be rewritten to equation 3.13.

$$d_{HATA} = 10^{\frac{119.39 - 44.49log_{10}(f_c) + 4.78log_{10}(f_c)^2 + 13.82log_{10}(h_t) + a(h_r)}{44.9 - 6.55log_{10}(h_t)}} \quad [m] \tag{3.13}$$

For the 3GPP RM LOS equation 3.7 can be rewritten to equation 3.14.

$$d_{RM}^{LOS} = 10^{\frac{PL_{RMa2}^{LOS} - PL_{RMa1}^{LOS}(dBP) + 20log_{10}(dBP)}{40}} \tag{3.14}$$

For the 3GPP RM LOS equation 3.10 can be rewritten to equation 3.15.

$$d_{RM}^{NLOS} = 10^{\frac{PL_{RMa}^{NLOS} - 162 + (24.37 - 3.7(h_b/h_t))^2 log_{10}(h_t - 20log_{10}(f_c) + (3.2log_{10}(h_t)) + 4.97)}{43.42 - 3.1log_{10}(h_t)} + 3} \tag{3.15}$$

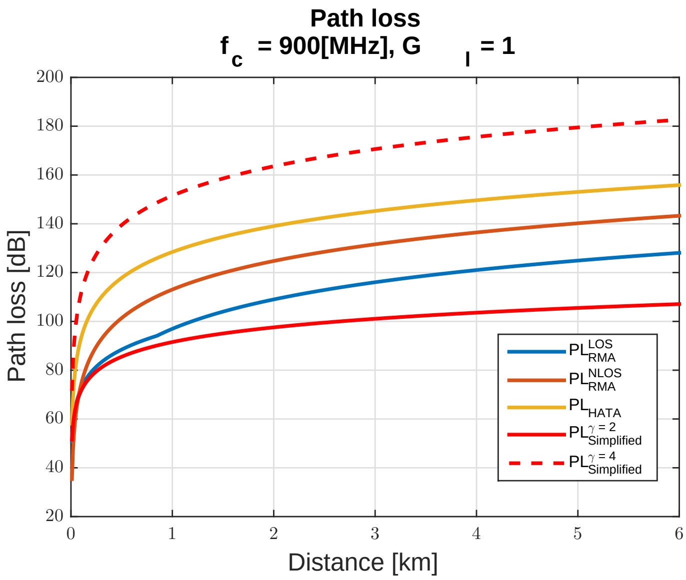

Figure 3.1: Path loss for the four models presented in this chapter, simplified, Hata and RMa

In table 3.3 the calculate coverage distance is given for the link budget shown in section 2.4. The result is given with penetration loss of 0 and 22 dB.

Coverage distance		
Variable	$L_{TP} = 0$	$L_{TP} = 22$
$d^{\gamma=2}_{simplified}$		
$d^{\gamma=4}_{simplified}$	0.73	0.23
d_{HATA}	3.6	0.85
d^{LOS}_{RM}		5.33
d^{NLOS}_{RM}		2.16

Table 3.3: Coverage distance for the models, the distance is given in meters

Chapter 4

Simulations

In this chapter a description of the simulation environment will be presented based on the link budget shown in section 2.4. The simulation will be able to calculate the expected received power for a random location based on the location of the BS. In chapter 2 the mobile coverage was discussed and it was seen that the receive power was influenced by the distance between transmitter and receiver and the carrier frequency in section 2.1.1. The actual gain of the antenna is influenced by the azimuth and elevation angle from the BS to the UE as discussed in section 2.1.3. The calculation of distance, azimuth and elevation angle will be described in section 4.2 of this chapter. The different propagation models that will be used in the simulation environment is discussed in chapter 3 and the implementation is given in section 4.3.

4.1 Base station sector

The sector of the BS will be the foundation of the simulation environment with each sectors having different setups regarding location, height, tilt, and azimuth. The setup of the sector will be used to calculate the path loss and receive power for locations around the position of the BS. A list with known information about certain BS around the location of the measurements have been given by Telenor for use with this project. Each BS have two or three sectors in the given area, and for each sector table 4.1 is showing the information that was given for each sector.

Sector information	
Longitude	[°]
Latitude	[°]
Transmit power	[dBi]
Azimuth	[°]
Elevation	[°]

Table 4.1: Base Station - details

The simulation will have root in the setup of the BS, with calculation of distance and bearing to all location points of the UE.

4.1.1 Calculation of the gain

Equation 2.6 can be formulated as in equation 4.1[21, p. 67]

$$G(\theta,\phi) = G_{az}(\phi) + G_{el}(\theta) \tag{4.1}$$

Where $G_{az}(\phi)$ is the gain in the azimuth plane for the angle ϕ and $G_{az}(\theta)$ is the gain in the elevation plane for the angle θ. From Athley et. el. [22] a formula for calculating the gain based on theoretical pattern for the azimuth- and elevation plane is used. The gain is calculated based on equation 4.2, 4.3 and 4.5.

$$G_{az}(\phi) = max(-12\left(\frac{\phi}{HPBW_{az}}\right)^2, SLL_{az}) \tag{4.2}$$

$$G_{el}(\theta) = max(-12\left(\frac{\phi}{HPBW_{el}}\right)^2, SLL_{el}) \tag{4.3}$$

$$\tag{4.4}$$

Where the SLL is the sidelobe level for the given plane. From the data sheet [14] the sidelobe level for the two planes is given as SLL_{az} = -25 dB and SLL_{el} = -18 dB. The gain in the azimuth and elevation is given relative to 0 [dB]. To relate it to a certain transmit power equation 2.6 is evaluated as in equation 4.5.

$$G(\theta,\phi) = max(G_{az}(\phi) + G_{el}(\theta), SLL_0) + G_0 \tag{4.5}$$

Where G_0 is related to the transmit power and SLL_0 is the sidelobe level depending on the characteristic of the antenna. SLL_0 = -30 is taken from the article [22]

4.2 Simulation trigonometry

In this section a description of the simulation environment will be given for the calculation of distance and bearing seen from the BS. In figure 4.1a the situation is illustrated from the side view and in figure 4.1b from above.

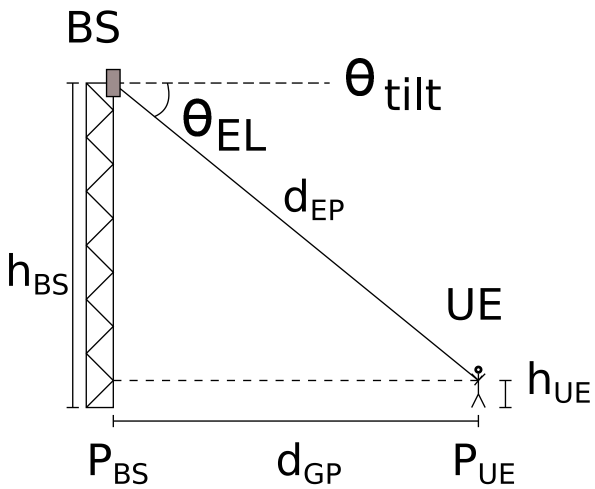

(a) Elevation angle, θ_{EL}, from the BS to the measurement point, M#. $\theta_0 = 90$.

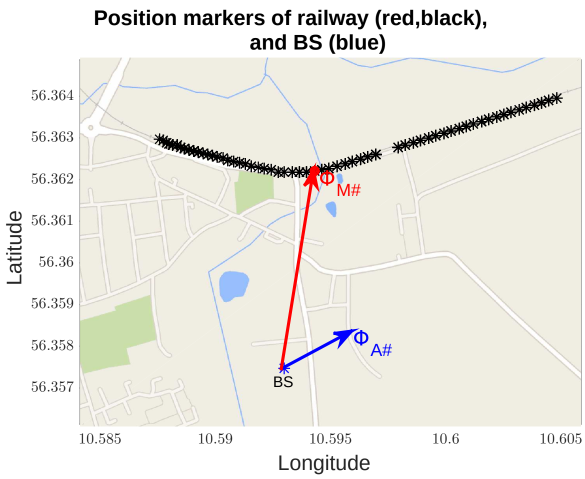

(b) Azimuth angle, ϕ_{AZ}, between the direction of $\phi_{A\#}$ and $\phi_{M\#}$. Where $\phi_{A\#}$ is the antenna pointing direction and $\phi_{M\#}$ is the angle from the BS to a measurement point,M#.

Figure 4.1: Figures showing the azimuth and elevation cases

In section 4.2.1 the calculation if the distance between two positions is given e.g. BS and UE and in section 4.2.2 the height difference between the BS and UE is included in the distance. In section 4.2.3 the angle between the pointing direction of the antenna and the position of the UE is given. The elevation angle is given in section 4.2.4.

4.2.1 Distance on the earth

The distance is calculated between two locations using the decimal degrees of longitude and latitude position in radians. The calculation of distances between two locations on earth is performed with the great circle distance calculation [23]. For great circle distances the earth is approximated as a sphere. The following derivation will be based on two arbitrary locations p_1 and p_2. The two locations $p_1(\varphi_{p1},\nu_{p1})$ and $p_2(\varphi_{p2},\nu_{p2})$, where φ is the latitude and ν is the longitude in radians.
The distance is calculated based on the radius of earth, r_{earth}, and the central angle, Θ_{CA}, shown in equation 4.6.

$$d_{GP} = r_{earth} \cdot \Theta_{CA} \tag{4.6}$$

The central angle, Θ_{CA}, between the two locations is found using the spherical law of cosine shown in equation 4.7.

$$\Theta_{CA} = acos\left(sin(\varphi_{p1})sin(\varphi_{p2}) + cos(\varphi_{p1})cos(\varphi_{p2})cos(\triangle\nu)\right) \tag{4.7}$$

Where $\triangle\nu = \nu_{p2} - \nu_{p1}$. The use of the cosine can result in rounding errors due to the floating-point precision. Because of these errors the Haversine function [24] are normally used, which are better conditioned. The Haversine is defined as in equation 4.8.

$$haversin(\Theta_{CA}) = sin^2\left(\frac{\Theta_{CA}}{2}\right) \tag{4.8}$$

Where Θ can be an arbitrary number in radians. The formula for the central angle can then be rewritten into equation 4.9. Then by the use of equation 4.6 the distance is found.

$$\Theta_{CA} = 2 \cdot arcsin\left(\sqrt{haversin(\phi_2 - \phi_1) + cos(\phi_1)cos(\phi_2)haversin(\lambda_2 - \lambda_1)}\right) \tag{4.9}$$

The error of using a spherical earth is 0.5 % for the latitude and 0.2 % for the longitude [25]. These errors have been found acceptable for use in this report. For better approximation the Vincenty formula can be used [26] which approximate the earth as a spheroid.

4.2.2 Distance - antenna to UE

The actual distance that the signal is travelling in a direct line between the BS and the UE is influenced by the curvature of the earth. In the calculation of this distance a simplification is used stating that the distances is so short that this can be left out and Pythagoras can be used. This simplification of the distance from the antenna to the UE is illustrated as the distance, d_{EP}, in figure 4.1a. The distance calculated in section 4.2.1 is treated as if the earth was a plane. In equation 4.10 the formula for the simplification is shown.

$$d_{EP} = \sqrt{d_{GP}^2 + (h_{BS} - h_{UE})^2} \tag{4.10}$$

4.2.3 Azimuth

The angle $\phi_{M\#}$ is found using the function azimuth in Matlab and the angle $\phi_{A\#}$ is given from Telenor. The two angles is both related two the same North heading. The azimuth angle found in this section is in relation to the antenna patterns as discussed in section **??**. In figure **??** the angle is plotted in a system of coordinates illustrating the situation seen in figure **??**. Because the antenna patterns is asymmetric it is necessary to keep track on which side of the antenna direction the measurement is performed. With the use of the atan2 function in Matlab this can be done simply as shown in equation 4.11.

$$\phi_{AZ} = atan2(sin(\phi_{diff}), cos(\phi_{diff})) \tag{4.11}$$

Where

$$\phi_{diff} = \phi_{A\#} - \phi_{M\#} \tag{4.12}$$

4.2.4 Elevation

The elevation angle is defined as in figure 4.1a and is found using Pythagoras as shown in equation 4.13.

$$\theta_{EL} = atan(h_{diff}/d) \tag{4.13}$$

where $h_{diff} = h_t - h_r$ and d is the distance from the BS to the measurement point.

In this section an explanation of how the different variables is calculated is given. The implementation of the bearing in the Matlab code is given in appendix A.1.

4.3 Simulation of the railway area

The simulation environment is build with base in the individual BSs. The layout of the BS and the antenna characteristics can be seen in section 4.1. The gain of the antenna can be calculated based on the bearing. The path loss models is based on the distance between transmitter and receiver. The receive power at any location around one of the sectors of the BS can be calculated based on the gain and the path loss model. The coverage in the area of the chosen railway stretch is simulated.

4.3.1 Coverage of the BSs

In figure 4.2 an example of the receive power is plotted for the area around the railway for one sector. The receive power in the example is calculated based on the 3GPP RM LOS model.

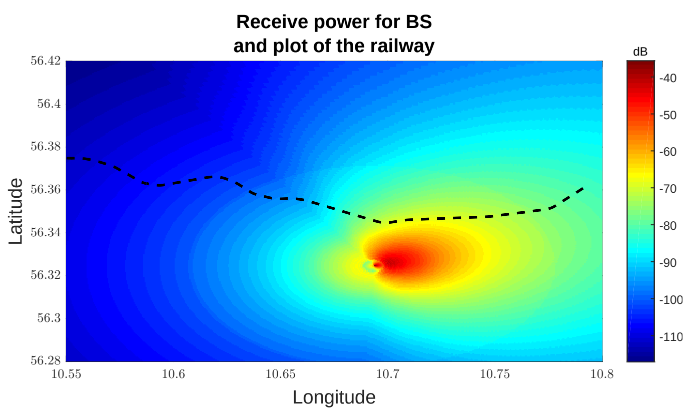

Figure 4.2: Coverage map showing the receive power for one BS in the railway surrounding

A complete grid with all sectors of the BSs is plotted in figure 4.3. The receive power in this example is plotted as the maximum receive power for each sector, based on the 3GPP RM LOS model. Similar grids can be simulated based on the other models explained in chapter 3.

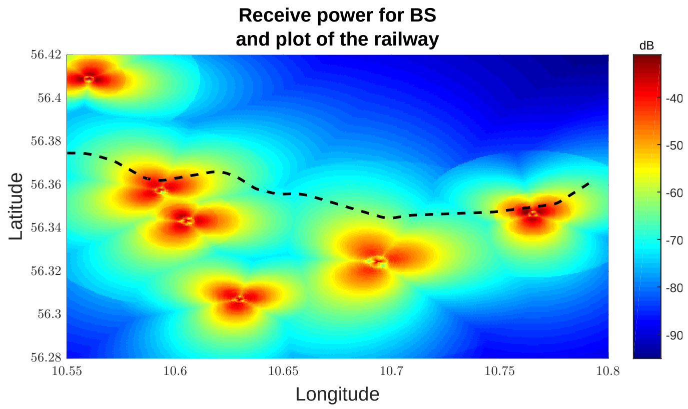

Figure 4.3: Coverage map showing the maximum receive power for all BSs in the railway surrounding

The area coverage probability can be found for the calculated received power in the grid according to the propagation models. The difference between the received power and the minimum requirements for the received power according to the link budget, can be used to plot the area coverage probability. The difference can be calculated as in equation 4.14.

$$P_{diff} = P_{LB} - P_r^{model} \tag{4.14}$$

The difference is plotted in figure 4.4 for the different path loss models. The line that goes through zero is showing the point for where the result is at the minimum requirement according to the link budget.

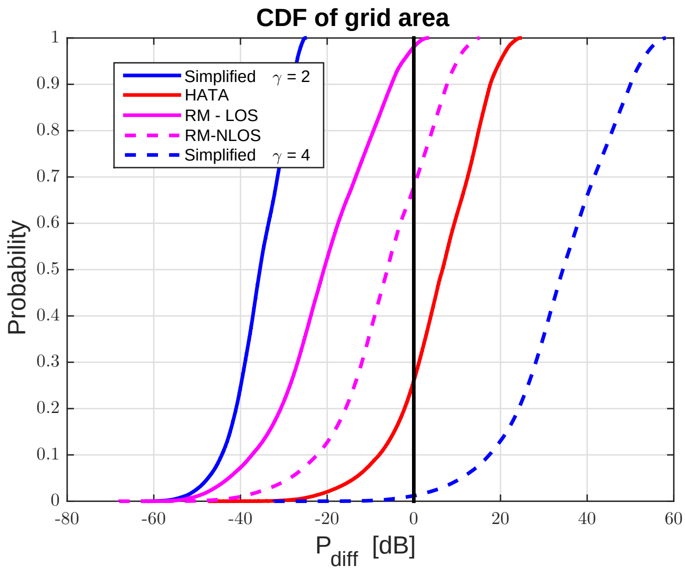

Figure 4.4: CDF of the grid power difference between P_r^{model} and P_{LB}

Area coverage probability	
Simplified $\gamma = 2$	100 %
Simplified $\gamma = 4$	12 %
HATA	26 %
RM LOS	98 %
RM NLOS	68 %

Table 4.2: Area coverage probability - for the simulation of the grid

The area coverage probability of the grid shows the difference between the models and that depending on the environment the path loss can be very different. The actual coverage in the grid can be different, as the BS simulated is the one with known information. The area around the railway seems to be covered by the known BS and in the following section simulation will be given.

4.3.2 Coverage along the railway

The coverage of the railway stretch will be discussed in this section. In figure 4.5 an example of the railway with the receive power according to the 3GPP RM LOS model is shown. The receive power is plotted onto a area map, with a colour scheme showing the receive power in dB.

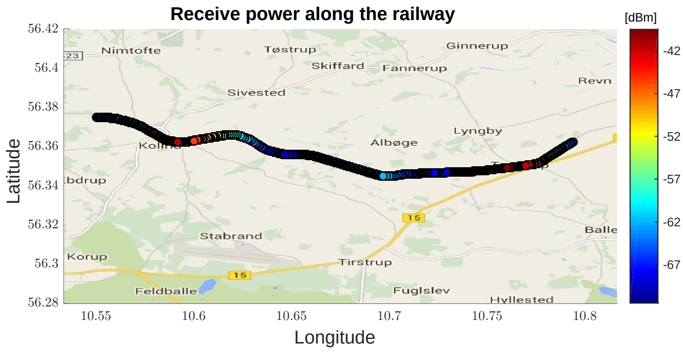

Figure 4.5: Receive power for all BSs in the railway surrounding

As in the grid a CDF is created for the different models, showing the difference according to equation 4.14. The CDF of the railway is shown in figure 4.6, for the link budget with train penetration loss of 0 [dB].

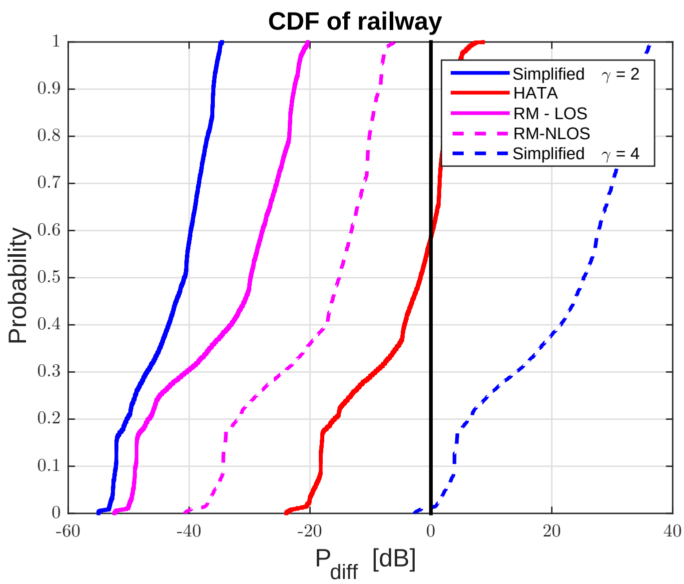

Figure 4.6: CDF of the railway power difference between P_r^{model} and P_{LB}

The results shows that the HATA model have lack in the coverage for the railway. The probability is given in table 4.3. The coverage probability for the case with a penetration loss of 20 [dB] is shown in figure 4.7.

Coverage probability	
Simplified $\gamma = 2$	100 %
Simplified $\gamma = 4$	1%
HATA	55 %
RM LOS	100 %
RM NLOS	100 %

Table 4.3: Area coverage probability - for the simulation of the railway

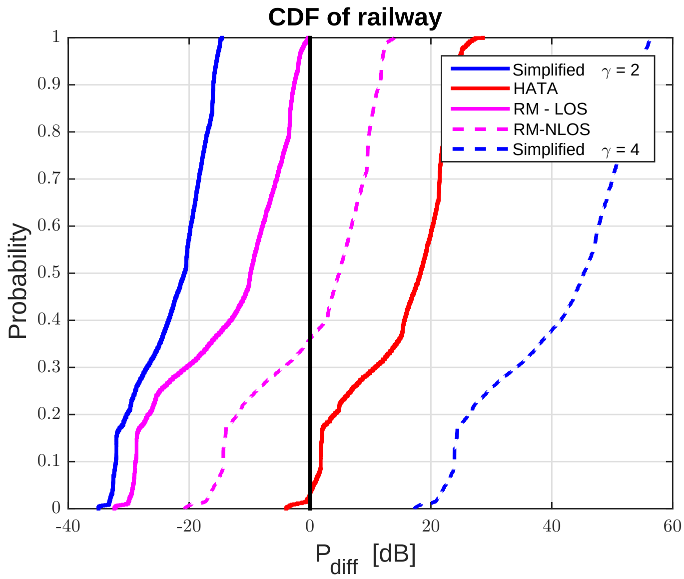

Figure 4.7: CDF of the railway power difference between P_r^{model} and P_{LB}

The results shows that the HATA model have lack in the coverage for the railway. The probability is given in table 4.4.

Coverage probability	
Simplified $\gamma = 2$	100 %
Simplified $\gamma = 4$	0%
HATA	2.5 %
RM LOS	100 %
RM NLOS	59 %

Table 4.4: Area coverage probability - for the simulation of the railway

4.4 Simulation results

The simulation have given an prediction on how the coverage of the area and of the railway is. The area coverage cannot be conclusive because of the possibility that BSs exist further above the railway. But because of the distance from the railway to the boundary of the grid it is expected that the coverage for the railway is not inflicted from this. The coverage of the railway shows that there can be a problem even if the train penetration loss is 0 [dB]. Two of the model even shows that the coverage along the railway is approximately 100 % not considering shadowing. With a penetration loss into the train of 20 [dB] the case is that the HATA model is almost showing a coverage of 0 and the RM NLOS is showing a coverage of around 60 %. With only the RM LOS model showing a coverage of nearly 100 %.

In the next chapter measurement along the railway inside and outside of the train will be investigated. A comparison between the inside and outside measurement will be given to get an penetration constant for penetration into the train. In chapter **??** a comparison between the measurement and the simulated will be given with a prediction of the penetration loss according to a model and the measurement along the railway.

Chapter 5

Measurements

In this chapter a description and an analysis of the measurements will be given. The measurements have been performed in the area of the two cities Kolind and Trustrup. The same area for which the simulations have been performed in chapter 4. The simulations shows a theoretical coverage and receive power along the railway. The measurements will give empirical results for comparison with the simulations.

5.1 The performed measurements

Two types of measurements have been taken along the railway, one inside the train and one outside of the train. The measurements inside of the train is expected to be affected by the penetration of the signal into the train. And the one taken outside of the train to be used as a reference of how the signal level is outside of the train. The measurements have been taken with a mobile phone to give an indication of how the signal level will be according to the UE. The measurements for the power received is the Received Signal Code Power (RSCP) value, which is measured on the Control Pilot Channel (CPICH)[27]. The phone measures the receive power for different sectors at the time which gives more data for the analysis. This will be seen for the investigation of the penetration loss in section 5.3.

5.1.1 Measurements inside the train

The measurements inside of the train have been performed between the two cities Kolind and Trustrup. This stretch is similar to the railway track seen in the simulations. The measurements have been given by the supervisor of the project, but a brief summary of how the measurements was taken have been given. The mobile phone have been placed on a table inside the train. The phone have not been used when the measurements have been taken except for a few brief checks of the software running. The measurement location for the train data is plotted in figure 5.1.

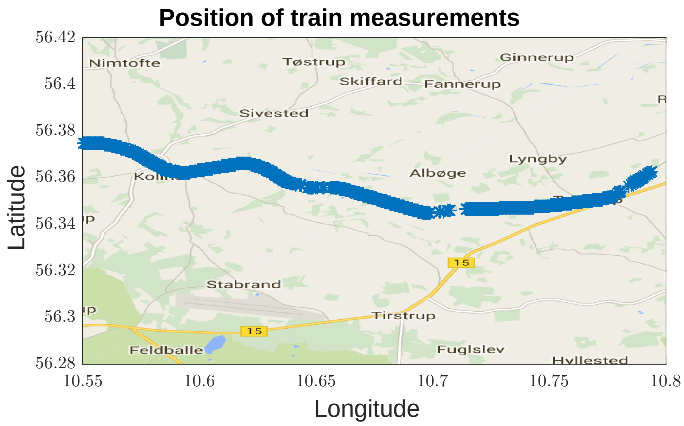

Figure 5.1: Measurement locations for the data inside the train

5.1.2 Reference route

The reference route have been measured outside of the train along two stretches where the road is going close to the railway. The measurements have been performed with the phone hold in the hand outside of the window of a driving car. In figure 5.2 the two stretches is plotted onto a map of the area.

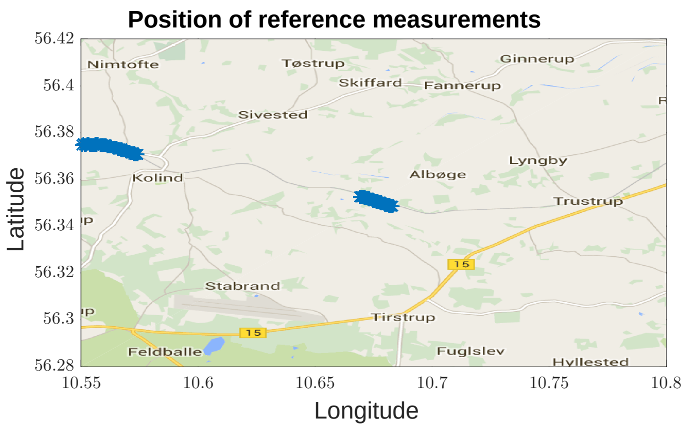

Figure 5.2: Measurement locations for the reference route

5.2 Incidence angle onto the train

In this section the calculation of the incidence angle onto the train is explained. How the direction of the train is calculated is discussed in section 5.2.2.

In figure 5.3 the BS, blue dot, is plotted in a map with one measurement point, red dot. The red line is plotted to help with the visualisation. Over the measurement point a train is plotted in gray with the direction of the train in the solid black line. The dotted lines from the measurement point is given the line perpendicular to the train direction and the the direction of the train in the opposite direction. The lines originated from the measurement point creates four quadrants which will be used to calculate the angle of incidence. The train is excepted to be symmetrical around the measurement point.

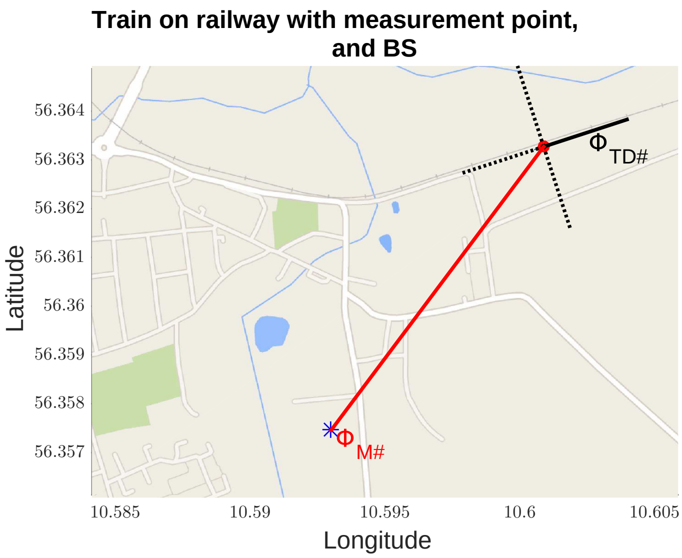

Figure 5.3

The angle between the direction of the train and the angle between the BS and the measurement point both originate from the measurement point when both angles is calculated based on the North heading. The angle between the two can then be found using the dot product as shown in equation 5.1.

$$\phi_{IA} = acos\left(\frac{dv_{\phi_M} \bullet dv_{\phi_{TD}}}{\| dv_{\phi_M} \| \| dv_{\phi_{TD}} \|}\right) \tag{5.1}$$

Where $\bullet$ is the dot product, ϕ_{IA} is the incidence angle, dv_{ϕ_M} is the direction vector between the BS to the measurement point and $dv_{\phi_{TD}}$ is the direction vector for the direction of the train. To relate it to the case with the four quadrant then if the angle is larger than 90°the result is subtracted from 180°.

5.2.1 Angle between measurement and BS

The angle between the measurement and the BS is calculated as described in in section 4.2 for the bearing. For simplicity the function in Matlab called "distance" is used. This function can find the angle between to point on the surface on earth.

5.2.2 Direction of the train

In this section the calculation of the train direction will be discussed in details. The direction of the train is used for the calculation of the incidence angle into the train. The calculation will be based on a north pointing coordinate system as the azimuth calculation in section 4.2.3.

The orientation of the railway is calculated based on Global Positioning System (GPS) data points along the track. Because the low precision of the position from the GPS a filter has to be applied to the data for a reliable approximation of the direction. In figure 5.4 an example of how the GPS position bounces in different direction can be seen.

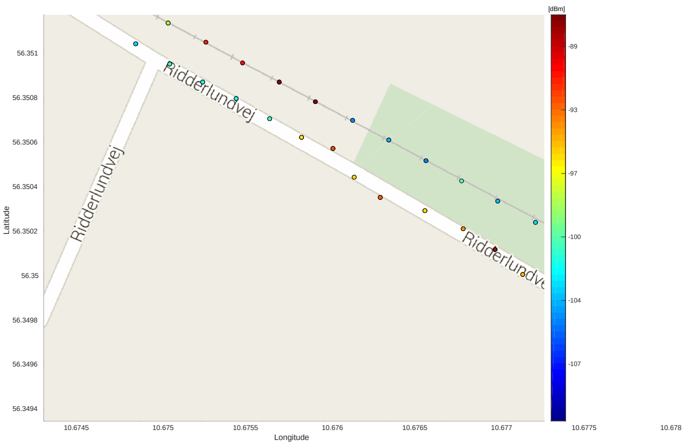

Figure 5.4: Example of how the GPS position is bouncing

The direction of the train is calculated based on the measurements, with a moving average. Where it takes 8 different samples and making and average of the angle that is calculate individually between sample 1 to 2, 2 to 3, 3 to 4 and so on.

5.3 Penetration loss into train

In this section a comparison between the measurement inside the train and the two reference stretches will be conducted. Reference route 1 is plotted in figure 5.5. The train data that follow the reference route is also plotted into the figure.

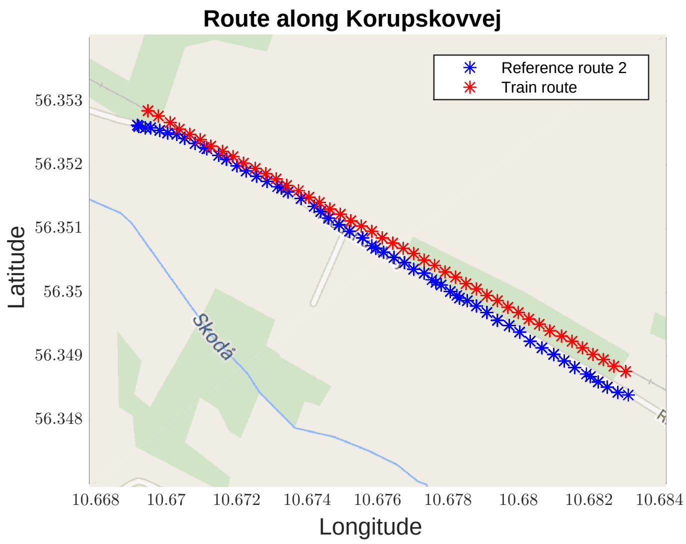

Figure 5.5: Plot of the data points before the shelter belt

For the same stretch the maximum receive power is plotted as a function of distance to the first measurement point for train and reference route respectively.

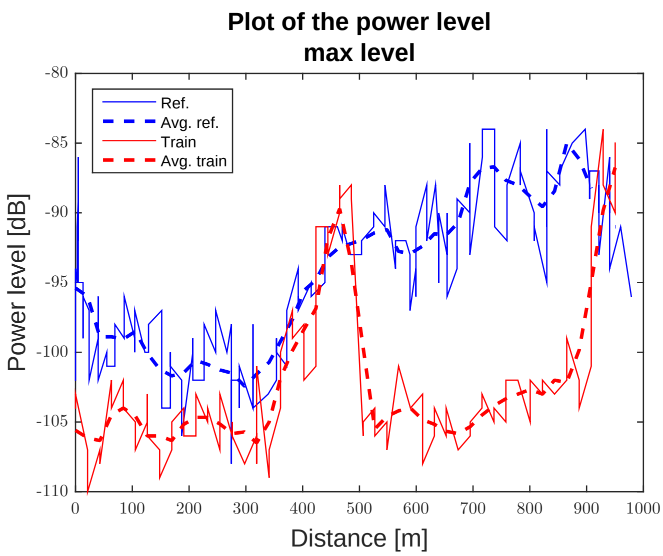

Figure 5.6: Figure of maximum RSCP values for the train- and reference route with average calculated value

From the power level it can be seen that the receive power for the reference route 1 starts to increase right before the shelter belt starts and stays high. For the train the same trend starts, but as the train enters the shelter belt the power level drops. In section 5.3.1 the data will be split into two routes one before and one inside the shelter belt for calculating the penetration loss. Reference route 2 is plotted in figure 5.7 along with the train data for the same stretch.

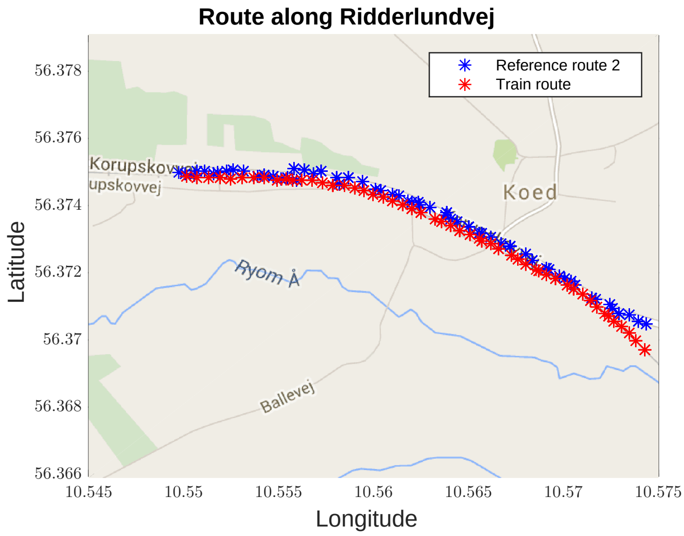

Figure 5.7: ridderlundvej1

For the same stretch the maximum receive power is plotted as a function of distance to the first measurement point for train and reference route respectively.

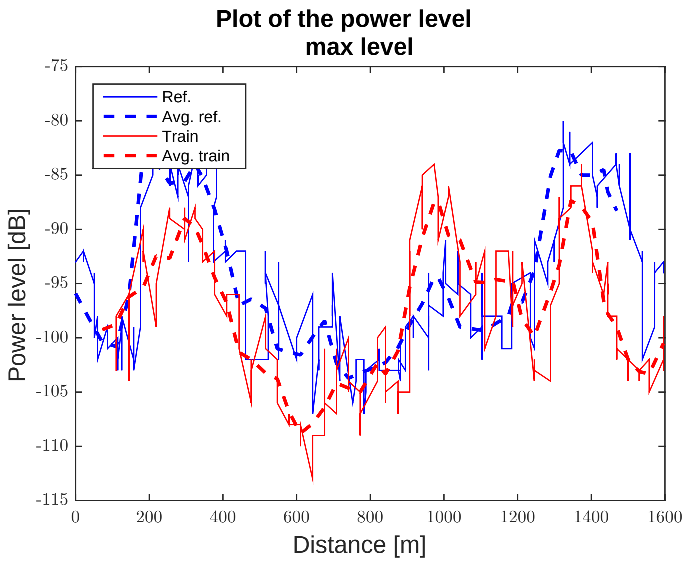

Figure 5.8: Figure of maximum RSCP values for the train- and reference route with average calculated value

In figure 5.8 it can be seen that the reference route and the train route is following the same trend. Around a distance of 900 the train routes receive power stays above the power level of the reference route for around 150 m. Expecting the area in Google maps it was found that the train and car route separates with a shelter belt in between. A closer look is plotted in figure 5.9.

Figure 5.9: Figure showing the shelter belt with the train and reference route

The penetration loss calculated along reference route 2 is discussed in section 5.3.2 and a conclusion on the penetration loss is given in section 5.4.

5.3.1 Penetration according to reference route 1

Penetration loss calculated along the stretch of route 1, the data is shown for the two cases before and inside the shelter belt. In figure 5.10 the data point is shown for the data before the shelter belt. These are the data that have been used to create the plot of the difference between the reference route and the train route.

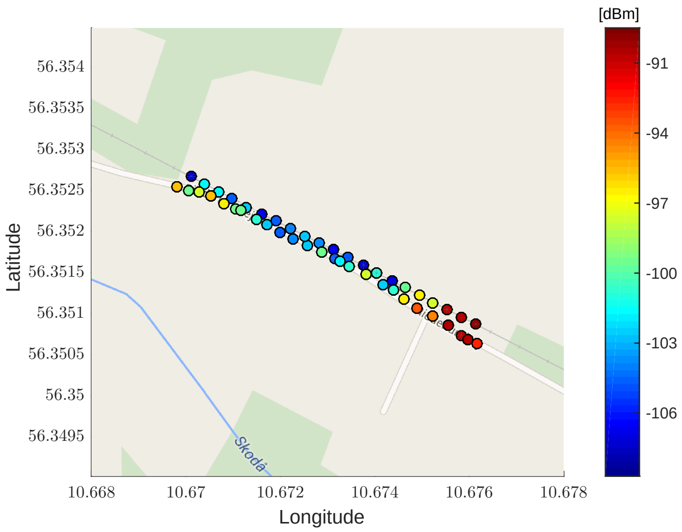

Figure 5.10: Plot of the data points before the shelter belt

In figure 5.11 the difference between the train data and the reference route is shown for four sectors. It can be seen that there is a difference between the lowest and highest mean value of approximately 4 dB for the incidence angle of around 70 degree. For the 50 degree incidence angle this value is approximately 2 dB.

Data for the route 1		
Sector	mean	std
38	2.95	2.6
42	6.27	3.7
100	7	2.9
340	4.07	3.4

Table 5.1: Comparison of reference route and train route

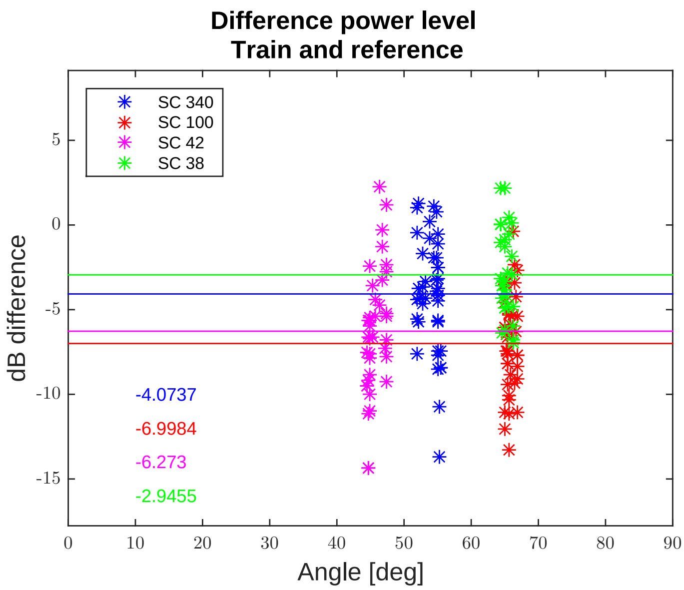

Figure 5.11: Difference between train- and reference route power level before the shelter belt.

The other case is in between the shelter belt shown in figure 5.12.

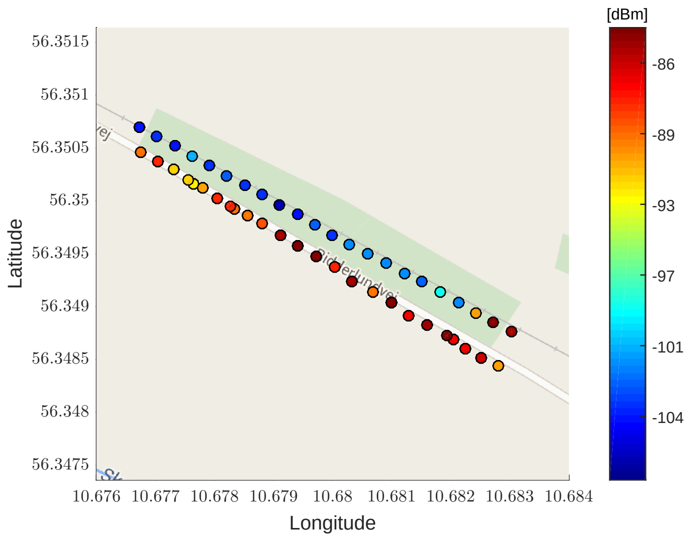

Figure 5.12: Plot of the data points inside the shelter belt

In figure 5.13 the difference between the train data and the reference route is shown for the four SCs. It can be seen that the average power level is quite lower in this area. This fact is interesting because it seem like a lot of the rail way is running through these kind of shelter belts or even forest.

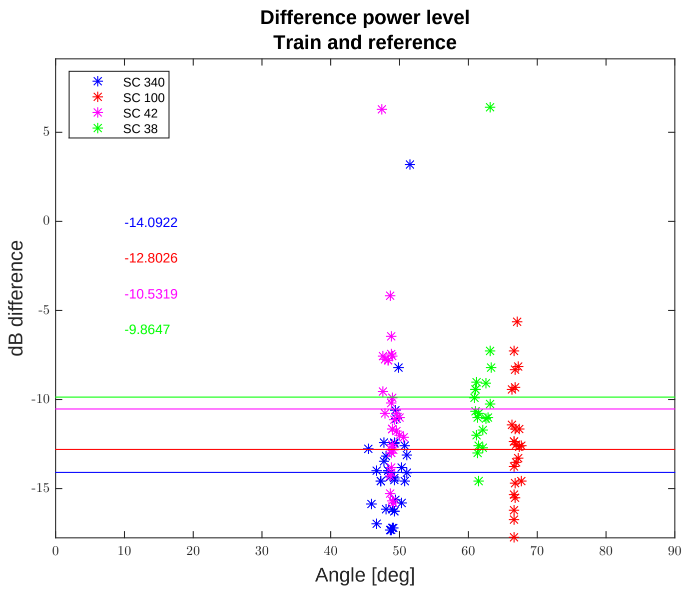

Figure 5.13: Difference between train- and reference route power level for the stretch on Ridderlundvej

Data for route 1		
Sector	mean	std
38	9.86	4.2
42	10.53	4.1
100	12.8	3.3
340	14.09	3.6

Table 5.2: Comparison of reference route and train route

5.3.2 Penetration according to reference route 2

In figure 5.14 the difference between the train data and the reference route is shown for the three SCs. It can be seen that the difference is around 5 - 6.4 dB if the problem area according to the discussion before is cut out. The results could indicate that there is a penetration loss around 5-6.5 dB. This corresponds to the results seen for the other route at least for the track before the shelter belt.

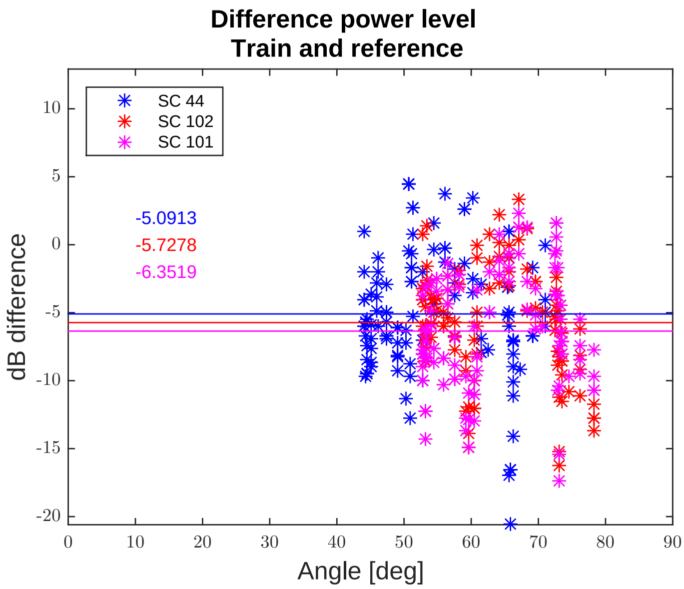

Figure 5.14: Difference between train- and reference route power level before the shelter belt.

Data for route 2		
Sector	mean	std
44	5.09	4.7
101	6.35	4.27
102	5.7	4.9

Table 5.3: Comparison of reference route and train route

5.4 Measurement conclusion

In section 5.3.1 and section 5.3.2 analysis of the penetration loss into the train is given. The penetration was analysed with respect to the incidence angle onto the train. From the data shown in figure 5.11 the penetration loss is calculated to be between 3 to 7 dB. The incidence angle is between 45 to 65 degrees. An relation between the incidence angle and the penetration loss have not been found. The result is quite similar to the result shown in figure 5.14, where the penetration loss is calculated to be between 5 to 6.4 dB. Also here a relation between the penetration loss and the incidence angle could not be found. For the last stretch on Korupskovvej, the part where the train is in between a shelter belt, seen in figure 5.13. The penetration loss is found to be between 9.8 to 14 dB. The results from route 1 and route 2 could give an indication of a penetration loss between 0 - 10 if there are no obstacles around the railway. And and rise in the penetration loss to between 0 - 20 if there are obstacles close to the railway.

Chapter 6

Conclusion

This report has highlighted a mobile coverage problem with the public transportation system when travelling by train. The initial investigation found that the train operators and the cellular operators have tried to come up with a solution for at least 8 years. The last article found gave the impression that a solution would come within 3 years. This project have tried to find a reason for the poor coverage inside the trains. It started with a examination of the mobile coverage and define a link budget. Investigation of different propagation models lead to the findings of coverage distances according to the the link budget and the propagation models.
Simulation of the railway in the area of Djursland, Denmark, found that the mobile coverage should be able to cover the railway track. At least for the case where the penetration loss into the train is 0 dB. The HATA model was the most pessimistic model and only covered 55 % of the railway. Both of the 3GPP RM models covered the track completely. If the penetration loss was raised to 22 dB according to the link budget the HATA model only covered around 2.5 % and the RM NLOS 59 %, still the most optimistic one covered almost 100 %.
The penetration loss got a significant part in from the simulation result and with measurements the actual penetration loss was found for two part of the railway. The investigation of the measurements found that two cases appeared one where the railway was covered behind a shelter belt and another where it was not. For the case where the railway was covered inside the shelter belt the mean penetration loss was around 10 - 14 dB with standard deviation between 3-4 dB. For the parts where the railway was free the penetration loss was between 3-7 dB, with a standard deviation of 2.6-4.9. Combining the two the penetration loss for the train will be between 0 - 20 dB for the measurements performed in this project.

6.0.1 Future work

There is still at lot of work that could be done to cover the aspect of the mobile coverage for the railway. An integration of the models and the propagation loss found in the report could give a tool for the prediction of the coverage inside the train. There is still some unanswered questions about the handover and obstacles close to the railway affecting the receive power of the signal. A more detailed measurement plan with the possibility to measure the penetration loss on a stationary train could help in the prediction of a precise model.

Appendix A

Appendix

A.1 Bearing

Two angles is calculated for each data point one for the azimuth and another for the elevation. The angles is used for the gain calculations as explained in section A.2. Information on the different cell towers is given in the cellTowers900.mat file. It is build as in table A.1. From

SC	Antenna direction	Tilt	Height	Latitude	Longitude
1	100°	2°	25 [m]	10.5900°	56.3465°
2	180°	4°	25 [m]	10.5900°	56.3465°

Table A.1: Structure of the CT information with and example

the measurements the scrambling code is given this is used to get the specific CT information belonging to each measurement point. A vector is created based on the measurement point and the CT of which it is connected to.

Code snippet A.1

Code snippet A.1: Code for calculating the azimuth and elevation angles

```
function varargout= bearing2(sc,posMeas,heightReceiver)

load cellTowers900.mat;
load dummyTower.mat; % BS dummy if no sc fits

cellTowers = [cellTowers900;cellTowerDummy];

dummy = 10000;
counterDummy = 1;
% Get the number of measurement points
numbMeas = length(sc);
% Find out which tower and direction the measurement connects to
 for i = 1:numbMeas
    connected = find(cellTowers(:,1) == sc(i));

    if connected
        indexNoDummy(counterDummy) = i;
        counterDummy = counterDummy +1;
    end

```

```
    if isempty(connected)
        connected = find(cellTowers(:,1) == dummy);
    end
```

A.1.1 Azimuth

The azimuth angle is calculated based on section 4.2.3. In code snippet A.2 the azimuth angle is calculated from the data points and the CT position. The angle is given around the direction of which the antenna is pointing. Clockwise is negative angle and counter clockwise is positive.

Code snippet A.2: The azimuth angle

```

 end
% Save the information based on the different towers (connetedTower)
% 2(azimuth),3(tilt),4(height),5(longitude),6(latitude)
towerPos = cellTowers(connectedTower,[5,6]);
towerInfo = cellTowers(connectedTower,[1,2,3,4]);
towerInfo(:,[5,6,7,8]) = NaN;
if heightReceiver(1,2) == 0
towerInfo(:,7) = 0;
else
    towerInfo(:,7) = cellTowers(connectedTower,7)-heightReceiver(:,2);
```

A.1.2 Elevation

The elevation angle is calculated based on section 4.2.4. In code snippet A.3 the elevation angle is calculated based on the height of the CT and the receiver and the distance from the CT the the measured point. The receiver height is set to 1.5 m. Code snippet A.2

Code snippet A.3: The elevation angle

```
towerInfo(:,8) = heightReceiver(:,1);
% towerInfo(:,2) = 90;
% Vector with the difference between the tower and the measurements
% vector = posMeas-towerPos;
% USE OF DISTANCE FUNCTION IN MATLAB
[distance_deg,azimuth_deg]=distance(towerPos(:,2),towerPos(:,1),posMeas(:,2),
    posMeas(:,1),'degrees');
vector = azimuth_deg;
% Calculate the azitmuth angle
phi = azimuth(vector,towerInfo);
[theta, dist] = elevation(towerPos,posMeas,towerInfo,heightReceiver);
%tilt_out = towerInfo(:,2);
```

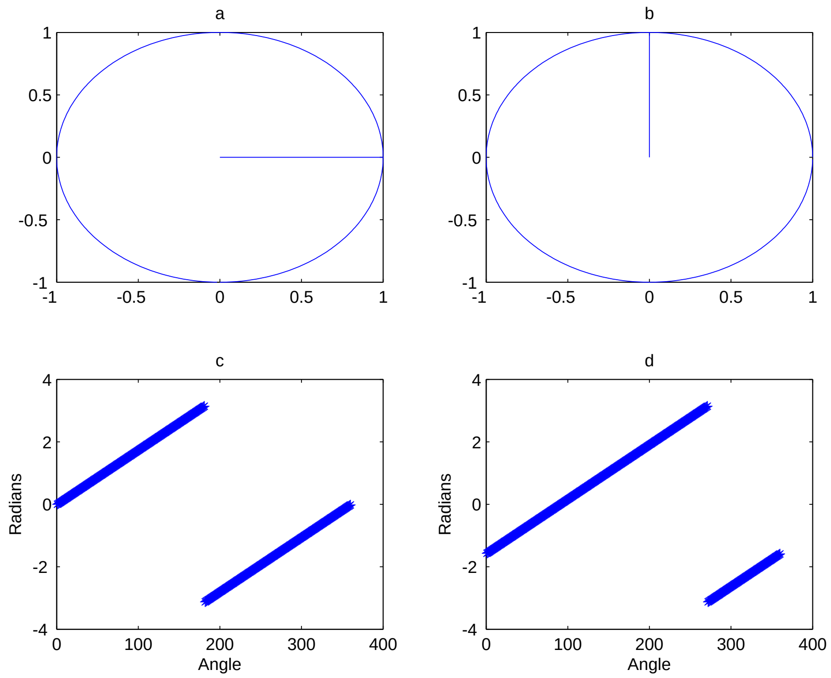

Figure A.1: Fig a and b: Circle with the antenna direction plotted. Fig c and d: Show the calculated angle in radians compared to the angle around the circle

A.1.3 Evaluation

To make sure that the azimuth angle is calculated correct and that the negative angle direction is clockwise a test is used. A circle is used from 0 to 2π, the result should give values in the range $(-\pi,\pi]$. The values should be focused around the direction the antenna is pointing. This can be seen in figure A.1. In subplot a and b the circle is plotted from [0,1] and the full 2 π round the direction of the antenna is plotted by the line. In subplot c and d the calculated radians is shown, c is associated with subplot a and d with b. In subplot c it can be seen that when turning from 0 to π on the circle that the values are positive, which correspond to counter clockwise from the cell tower up till 180 degree. The same can be seen in figure d, here it just starts in the negative area goes to the positive.

In figure A.2 the elevation angle is plotted compared with the distance. The difference between the CT and the MS is $h_{diff} = 28.5$ [m].

From the two figures it should be seen that the calculation of the two angles is done as proposed in section 4.2.

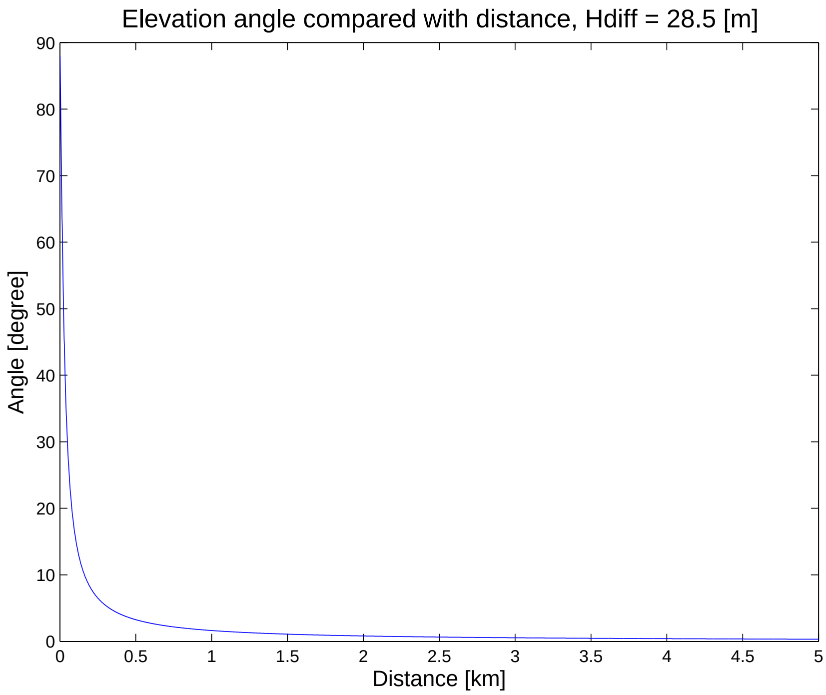

Figure A.2: Elevation angle compared with the distance

A.2 Gain calculations

The antenna gain is based on patterns for the azimuth and elevation plane. Patterns for six different tilt values is given in matrices with the pattern being spaced with 1 deg. In figure **??** the elevation and azimuth patterns are shown for tilt value of 0 and 10. In table A.2 a piece of the two matrices is shown. The values are losses, so a loss of 0 dB gives a maximum gain and as the loss increase the gain decrease. The initial gain for tilt $= 0$ is $G_{tilt:0} = 16.09$ and for tilt

Degree	0	1	2	3	4	5	6	7	8	9	10	11
Azimuth (tilt = 0)	0	0.01	0.02	0.04	0.06	0.1	0.13	0.18	0.24	0.3	0.36	0.44
Elevation (tilt = 0)	0	0.28	1.17	2.71	5	8.23	12.73	18.78	22.91	21.53	21.09	22.47
Azimuth (tilt = 10)	0.01	0	0	0	0.01	0.02	0.04	0.08	0.12	0.17	0.23	0.29
Elevation (tilt = 10)	38.31	30.3	23.24	16.92	11.89	8.01	5.06	2.86	1.32	0.38	0	0.17

Table A.2: dB values for the specific angle given the pattern of either 0 or 10 degree tilt.

$= 10$ is $G_{tilt:10} = 15.89$. The gain in the azimuth plane is quite similar which also can be seen in figure **??**, and from the table it is seen that the direction is just skewed with a few degrees. For the elevation it can be seen in table A.2 that for tilt $= 0$ that the maximum is at 0 degree and for tilt $= 10$ it is located a 10 degrees.

A.2.1 Script

The script created uses three vector to determine the gain from the five different patterns. It takes in a azimuth plane vector, elevation plane vector and tilt vector. The vector size of the three vectors correspond to the number of data points that needs to be calculated and should be the same size. The azimuth plane vector consist of angles in radians with the range $(-\pi,\pi]$ with the center around the direction of the antenna pattern. In section 4.2.3 a describtion of how the angle is calculated can be found. The elevation plane vector consist of angles in radians with the range $(0 : \pi/2)$ if the earth surface is considered plane. The vector is found based on section 4.2.4. The tilt vector is based on the tilt angles of the different towers of which each data point is connected. The tilt vector is found based on the measurements performed and the scrambling code recorded. In code snippet A.4 the indexing is found for the azimuth and elevation plane.

Code snippet A.4: Index based on the angles for both azimuth and elevation plane

```
function [out] = gain(phi,theta,tilt)
% load pattern_data;
%% calculates the gain.
phideg = round(phi*180/pi);
thetadeg = round(theta*180/pi);
degreeVector = 0:1:359;
% return the vector according to the index of the pattern to be sure to go
% in the right direction
for i = 1:length(phideg)
if sign(phideg(i)) == -1
    phideg(i) = 360+phideg(i);
end
% make an index vector for the azimuth and the elevation
indexPhi(i,1) = find(degreeVector(1,:) == phideg(i));
indexTheta(i,1) = find(degreeVector(1,:) == thetadeg(i));
end

% the two vectors put into a matrix.
angle = [indexPhi,indexTheta];

[gain,azimuth,elevation] = determinePattern(angle,tilt);
% Gain of all with the lowest possible gain to be -30 dB
out = max(gain + azimuth + elevation,-30);

out = out';


end
```

The indexes is used to calculate the gain of the initial, azimuth and elevation. This is done in code snippet A.5.

Code snippet A.5: Return gain for initial and azimuth and elevation

```
%% Returns pattern gains
% Function returning three vectors containing the initial, azimuth and
% elevation gain according to the tilt vector

function [gain,patternAzimuth,patternElevation] = determinePattern(angle,tilt)
load pattern_data;
for i = 1:length(tilt)

switch(tilt(i))

    case {0,1}
        % azimuth lowest possible gain -25
        patternAzimuth(i) = max(-pattern_tilt0(2,angle(i,1)),-25);
%         patternAzimuth(i) = -pattern_tilt0(2,angle(i,1));
        % elevation lowest possible gain -25
        patternElevation(i) = max(-pattern_tilt0(3,angle(i,2)),-18);
%         patternElevation(i) = -pattern_tilt0(3,angle(i,2));
        % initial gain
        gain(i) = gain_tilt0;
    case {2,3}
%         patternAzimuth(i) = -pattern_tilt2(2,angle(i,1));
%         patternElevation(i) = -pattern_tilt2(3,angle(i,2));
        patternAzimuth(i) = max(-pattern_tilt2(2,angle(i,1)),-25);
        patternElevation(i) = max(-pattern_tilt2(3,angle(i,2)),-18);

        gain(i) = gain_tilt2;
    case {4,5}
%         patternAzimuth(i) = -pattern_tilt4(2,angle(i,1));
%         patternElevation(i) = -pattern_tilt4(3,angle(i,2));

        patternAzimuth(i) = max(-pattern_tilt4(2,angle(i,1)),-25);
        patternElevation(i) = max(-pattern_tilt4(3,angle(i,2)),-18);

        gain(i) = gain_tilt4;
    case {6,7}
%        patternAzimuth(i) = -pattern_tilt6(2,angle(i,1));
%         patternElevation(i) = -pattern_tilt6(3,angle(i,2));
         patternAzimuth(i) = max(-pattern_tilt6(2,angle(i,1)),-25);
        patternElevation(i) = max(-pattern_tilt6(3,angle(i,2)),-18);
        gain(i) = gain_tilt6;
```

A.2.2 Evaluation

In figure A.3 to figure A.8 the gain pattern is plotted in a mesh structure with tilt values of 0:2:10. The distance is in km and is shown with the CT in [0,0], the antenna is pointing up in

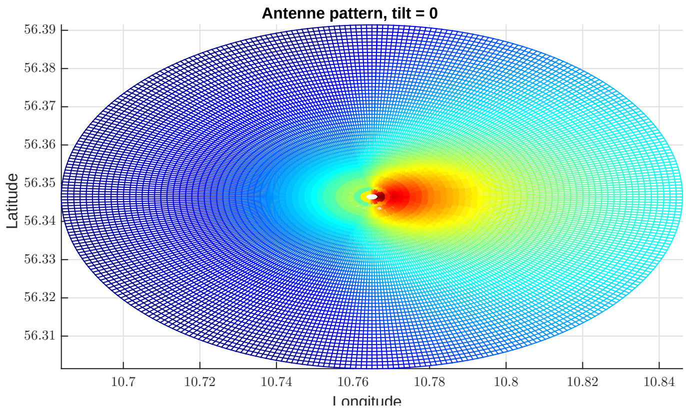

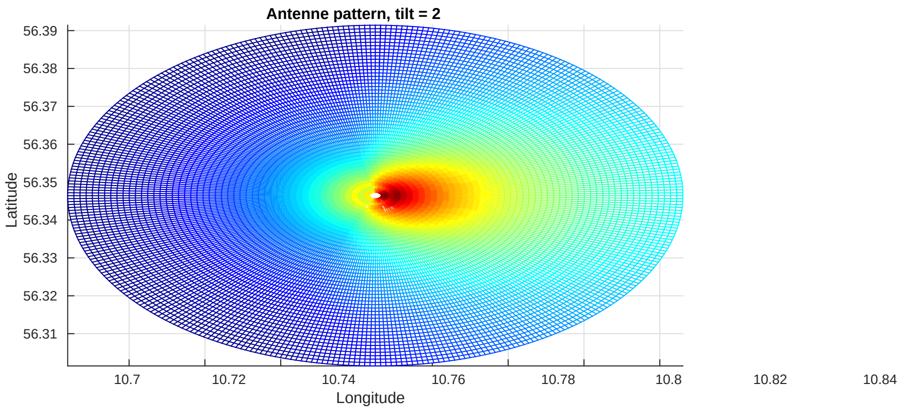

Figure A.4: Antenna gain for Tilt = 2

all cases. It can be seen that as the tilt is increasing the hot area is decreasing. The area behind the antenna is influenced by the tilt of the antenna, this is the reason for the difference in the power level in the six figures.

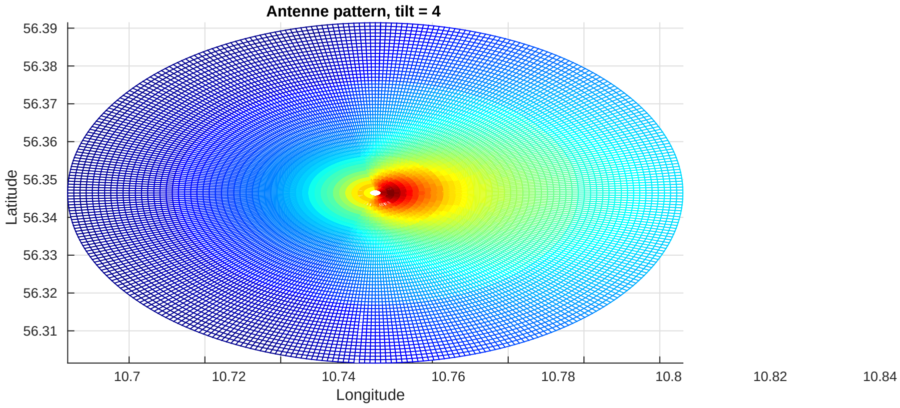

Figure A.5: Antenna gain for Tilt = 4

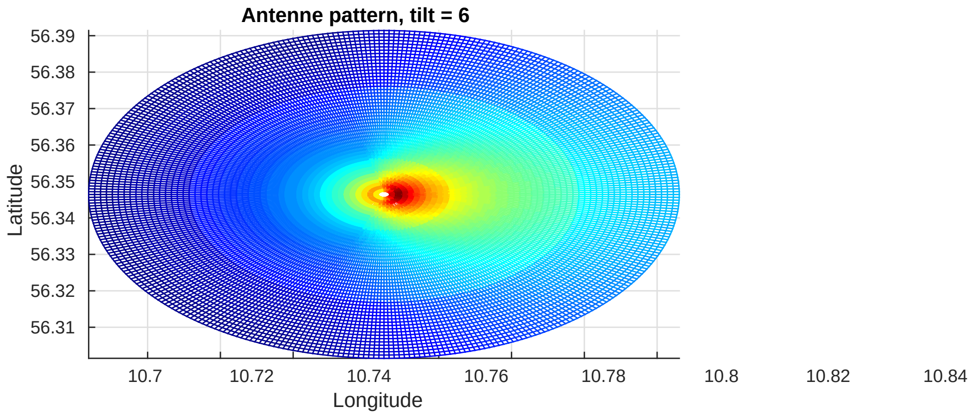

Figure A.6: Antenna gain for Tilt = 6

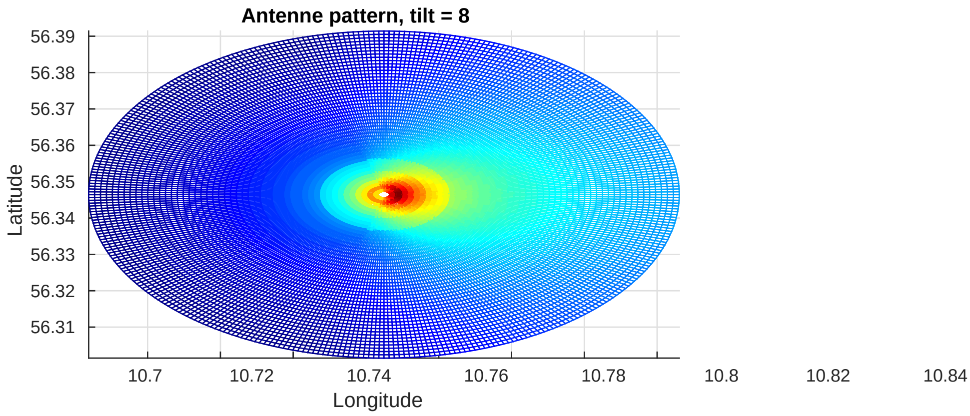

Figure A.7: Antenna gain for Tilt = 8

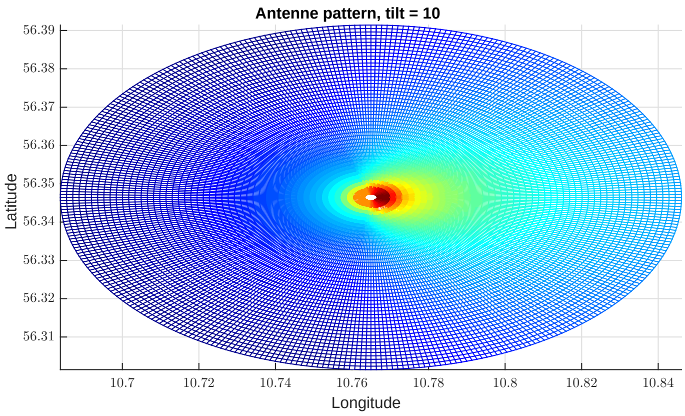

Figure A.8: Antenna gain for Tilt = 10

Acronyms

BS Base Station. 1, 3–5, 11, 13, 18–25, 27, 29, 30

CPICH Control Pilot Channel. 28

GPS Global Positioning System. 31

LOS Line-Of-Sight. 5, 14

MS Mobile Station. 13

NLOS No Line-Of-Sight. 14

RMa Rural Macro-cell. 14

RSCP Received Signal Code Power. 28

UE User Equipment. 11, 18, 20, 21, 28

Symbols

a correction factor for the height of the receiver based on the size of the coverage area, [dB]. 14

d distance between transmitter and receiver. 6, 14, 15

$d0$ reference distance, [m]. 13

d_{BP} break point distance, [m]. 14, 15

f_c carrier frequency, [Hz]. 6, 14

G_l product of the receive and transmit antenna field radiation patterns in the LOS direction, [.]. 6

γ path loss exponent, [.]. 13

h_b average building height, [m]. 15

h_r height of the receiver, [m]. 14, 15

h_t height of the transmitter, [m]. 14, 15

K constant dependent on antenna characteristics and channel attenuation, [.]. 13

λ wavelength. 6

P_L path loss, [dB]. 5

P_r power received, [dBm]. 5

P_t power transmitted, [dBm]. 5, 6

PL_{FS} free-space path loss, [.]. 13

$PL_{Hata}^{extended}$ extended Hata path loss for urban areas, [dB]. 14

PL_{Hata}^{rural} Hata path loss for rural areas, [dB]. 14, 16

PL_{Hata}^{urban} Hata path loss for urban areas, [dB]. 14, 16

PL_{RMa1}^{LOS} rural macro path loss for LOS before break point, [dB]. 15, 16

PL_{RMa2}^{LOS} rural macro path loss for LOS after break point, [dB]. 15, 16

PL_{RMa}^{NLOS} rural macro path loss for NLOS, [dB]. 15, 16

$PL_{Simplified}$ simplified path loss, [dB]. 13

W street width, [m]. 15

Bibliography

[1] Cisco. Cisco visual networking index: Global mobile data traffic forecast update, 2013–2018. Technical report, Cisco, February 2014. URL http://www.cisco.com/c/en/us/solutions/collateral/service-provider/visual-networking-ind

[2] Ericsson Research. Traffic and Market Data Report on the Pulse of the Networked Society. Technical report, Ericsson, November 2011. URL http://hugin.info/1061/R/1561267/483187.pdf.

[3] ITU. ICT FACTS AND FIGURES. Technical report, ITU, 2014. URL http://www.itu.int/en/ITU-D/Statistics/Documents/facts/ICTFactsFigures2014-e.pdf.

[4] Erhversstyrelsen. Mobilkortlægning 2013. Technical report, Erhversstyrelsen, 2013. URL https://erhvervsstyrelsen.dk/mobilkortlaegning-2013.

[5] M. K. Thomsen. Dsb vil forbedre mobil dækning i togene. http://ing.dk/artikel/dsb-vil-forbedre-mobil-daekning-i-togene-82048, 2007. Date: 5. October, Language: Danish.

[6] J Møllerhøj. Dsb erkender dårligere mobil-dækning i ic4-tog. http://ing.dk/artikel/dsb-erkender-darligere-mobil-daekning-i-ic4-tog-107193, 2010. Date: 11. March, Language: Danish.

[7] J Møllerhøj. Solfilm blokerer for mobiltelefoner i ic4-tog. http://ing.dk/artikel/solfilm-blokerer-mobiltelefoner-i-ic4-tog-107152, 2010. Date: 11. March, Language: Danish.

[8] J Møllerhøj. Nu kommer der hurtigere internet og bedre mobildækning i tog. http://ing.dk/artikel/nu-kommer-der-hurtigere-internet-og-bedre-mobildaekning-i-tog-129 2012. Date: 8. Maj, Language: Danish.

[9] J Møllerhøj. Dsb: Ja, der er problemer med wifi og telefoni i vores tog. http://ing.dk/artikel/dsb-ja-der-er-problemer-med-wifi-og-telefoni-i-vores-tog-135032, 2012. Date: 18. Dec, Language: Danish.

[10] J Møllerhøj. Sådan vil dsb fikse internetbøvl i toget. http://ing.dk/artikel/sadan-vil-dsb-fikse-internetbovl-i-toget-135541, 2013. Date: 15. January, Language: Danish.

[11] Mads Elkær. Dsb damper: Mobildækningen i danmark stinker. `http://www.computerworld.dk/art/229020/dsb-damper-mobildaekningen-i-danmark-stinker`, 2013. Date: 21. november, Language: Danish.

[12] Ulrik Andersen. Nu får togpassagerer endelig bedre internet og mobilforbindelse. `http://ing.dk/artikel/nu-faar-togpassagerer-endelig-bedre-internet-og-mobilforbindelse-` 2015. Date: 15. May, Language: Danish.

[13] Ieee standard definitions of terms for antennas. *IEEE Std 145-1993*, pages 1–32, April 2013. doi: 10.1109/IEEESTD.2013.6507364.

[14] Kathrein. Data sheet 800 10621.

[15] J.B. Andersen, T.S. Rappaport, and S. Yoshida. Propagation measurements and models for wireless communications channels. *Communications Magazine, IEEE*, 33(1):42–49, Jan 1995. ISSN 0163-6804. doi: 10.1109/35.339880.

[16] F. Abrishamkar and J. Irvine. Comparison of current solutions for the provision of voice services to passengers on high speed trains. In *Vehicular Technology Conference, 2000. IEEE-VTS Fall VTC 2000. 52nd*, volume 4, pages 1498–1505 vol.4, 2000. doi: 10.1109/VETECF.2000.886083.

[17] 3GPP. The mobile broadband standard. `http://www.3gpp.org/`, 2014. Seen: 6. October 2014.

[18] M. Hatay. Empirical formula for propagation loss in land mobile radio services. *Vehicular Technology, IEEE Transactions on*, 29(3):317–325, Aug 1980. ISSN 0018-9545. doi: 10.1109/T-VT.1980.23859.

[19] Andrea Goldsmith. *Wireless Communication*. Cambridge University, 1. ed. edition, 2005.

[20] 3GPP. Evolved Universal Terrestrial Radio Access (E-UTRA); Further advancements for E-UTRA physical layer aspects. TR 36.814, 3rd Generation Partnership Project (3GPP), March 2010. URL `http://www.3gpp.org/ftp/Specs/html-info/36814.htm`.

[21] Constantine A. Balanis. *Antenna Theory: Analysis and Design*. Wiley-Interscience, 2005. ISBN 0471714623.

[22] F. Athley and M.N. Johansson. Impact of electrical and mechanical antenna tilt on lte downlink system performance. In *Vehicular Technology Conference (VTC 2010-Spring), 2010 IEEE 71st*, pages 1–5, May 2010. doi: 10.1109/VETECS.2010.5493599.

[23] John P. Snyder. *Map Projections: A Working Manual*. Geological Survey (U.S.), 1987.

[24] Roger W. Sinnott. Virtues of the Haversine. *Sky Telesc.*, 68:159, 1984.

[25] TSO. *Manual of Navigation*. TSO, 1987.

[26] T. Vincenty. Survey review xxii, 1975.

[27] 3GPP. Physical layer; Measurements (FDD). TS 25.215, 3rd Generation Partnership Project (3GPP), September 2008. URL `http://www.3gpp.org/ftp/Specs/html-info/25215.htm`.